Title
Neural recording and modulation technologies

Journal
Nature Reviews Materials, 2(2)

ISSN
2058-8437

Authors
Chen, Ritchie
Canales, Andres
Anikeeva, Polina

Publication Date
2017-02-01

DOI
10.1038/natrevmats.2016.93

Peer reviewed

HHS Public Access

Author manuscript

Nat Rev Mater. Author manuscript; available in PMC 2019 August 23.

Published in final edited form as:

Nat Rev Mater. 2017 February ; 2(2): . doi:10.1038/natrevmats.2016.93.

Neural Recording and Modulation Technologies

Ritchie Chen[1], **Andres Canales**[1], **Polina Anikeeva**[1]

[1]Department of Materials Science and Engineering, and Research Laboratory of Electronics, Massachusetts Institute of Technology, Cambridge, MA, USA

Abstract

Within the mammalian nervous system, billions of neurons connected by quadrillions of synapses exchange electrical, chemical and mechanical signals. Disruptions to this network manifest as neurological or psychiatric conditions. Despite decades of neuroscience research, our ability to treat or even to understand these conditions is limited by the tools capable of probing the signalling complexity of the nervous system. Although orders of magnitude smaller and computationally faster than neurons, conventional substrate-bound electronics do not address the chemical and mechanical properties of neural tissue. This mismatch results in a foreign-body response and the encapsulation of devices by glial scars, suggesting that the design of an interface between the nervous system and a synthetic sensor requires additional materials innovation. Advances in genetic tools for manipulating neural activity have fuelled the demand for devices capable of simultaneous recording and controlling individual neurons at unprecedented scales. Recently, flexible organic electronics and bio- and nanomaterials have been developed for multifunctional and minimally invasive probes for long-term interaction with the nervous system. In this Review, we discuss the design lessons from the quarter-century-old field of neural engineering, highlight recent materials-driven progress in neural probes, and look at emergent directions inspired by the principles of neural transduction.

(Web summary)

Understanding the dynamics and architecture of the nervous system requires tools for recording and modulating billions of neurons. This article reviews the history of neural engineering and the materials innovation at the interface between neural tissue and synthetic sensors.

Introduction

Understanding the information transfer and processing within the mammalian nervous system is one of the most urgent challenges faced by the biomedical community. Neurological, neurodegenerative, psychiatric, and neuromuscular conditions, for example, Parkinson's disease, Alzheimer's disease, major depressive disorder, and multiple sclerosis, respectively, affect an ever-increasing percentage of our aging population (Fig. 1a–b) [1–3], and traumatic injuries to the nervous system contribute 2.4 million patients each year to the

Correspondence to P. A., anikeeva@mit.edu.

Competing financial interests

The authors declare no competing financial interests.

disability burden in the US alone [4]. Furthermore, inflammatory conditions, such as hypertension and arthritis, have been linked to changes in peripheral nerve activity [5]. Although basic neuroscience research of the past century has greatly advanced our understanding of neuronal function, the ability to record and manipulate the dynamics of the nervous system remains insufficient to treat these psychiatric and neurological disorders or to restore function following nerve injury.

Within the 1.3 litre volume of the human brain, billions of neurons, divided into thousands of genetically and structurally defined subtypes, communicate with each other through quadrillions of synapses (Fig. 1d–g) [6]. Notably, neurons represent only ~50% of the cells in the brain. The other half are electrically inactive glia that include astrocytes, oligodendrocytes and microglia,[7] the roles of which in brain function remains an active area of research [8, 9]. Similarly, the ~45-cm long, 1.5-cm thick spinal cord encompasses a variety of motor and interneurons, Schwann cells, and neuronal processes connecting the brain to the >150,000 km web of the peripheral nervous system [10] (FIG. 1h–j).

Neural activity is marked by millisecond-long 80–100 mV spikes in cell-membrane voltage called action potentials [6]. Aided by voltage-sensitive ion channels, action potentials propagate across neural membranes to release neurotransmitters into the synaptic cleft. Neurotransmitter uptake by the dendrites of synaptic partners results in signal transduction. In addition to chemical and electrical signals, neurons can respond to physical stimuli, such as pH [11], temperature [12, 13], pressure and tension [14] mediated by a variety of ion channels. Understanding neural function hence requires tools that can communicate with neurons across the diversity of their signaling capacities.

Driven by Moore’s law over the past 25 years, miniaturization of electronic devices down to the nanoscale has delivered unprecedented computational power. Although neuroprosthetic research has undoubtedly benefitted from these advances, additional design parameters need to be included for effective long-term operation and clinical translation of neural interfaces. The complexity of neural tissue requires further materials innovation beyond microfabricated semiconductor circuits. Consideration of the brain’s mechanical, electrical and chemical properties, and the diversity of neural signaling pathways may guide materials design to establish intimate long-term synthetic interfaces capable of faithful recording and stimulation of neural activity.

History of neural engineering

From neuroscience to neural engineering.

Motivation to answer fundamental questions in neuroscience has consistently inspired the invention of new technologies (FIG. 2). In the 1950s, wires were introduced to measure electrical activity in the nervous system [15], followed by patch-clamp electrophysiology in the 1970s [16] to elucidate synaptic transmission. In the 1980s to 1990s, silicon multielectrode arrays [17, 18], and stereotrodes and tetrodes [19, 20] have been developed to investigate communication between large groups of neurons within distinct neural circuits.

These probe innovations relied on tailoring device geometry and electrical impedance to a particular neuroscience application. For extracellular recordings, the impedance is determined by the capacitive characteristics of the interface between the electrode and the cerebro-spinal fluid, which is a function of the electrode material and the tip area. High-impedance electrodes (5–10 MΩ) are typically used to record action potentials with high signal-to-noise ratios (SNR > 20) from neurons within a 10-μm radius [21]. Insulated steel, tungsten, gold and platinum microwires with dimensions of approximately 10–100 μm and impedances of less than 1 MΩ are commonly employed for extracellular recordings from moderate numbers of neurons [22]. Stereotrodes and tetrodes consist of 2 or 4 polymer-insulated 12-μm nickel–chromium (NiCr) microwires that are electrochemically coated with gold to lower the impedance from about 1–3 MΩ to 100–500 kΩ and to improve biochemical stability [19, 20]. The close proximity of multiple microwires enables deconvolution of overlapping population signals to identify action-potential shapes corresponding to specific cells via principal component analysis [23]. Neurotrophic electrodes integrate a microwire within a pipette carrying neurotrophic factors that stimulate neuronal ingrowth for high-fidelity recordings [24].

Microfabricated neural probes.

By the 1980s, advances in semiconductor microfabrication led to the development of silicon-based multielectrode arrays known as Utah arrays [17] and Michigan probes [18]. Utah arrays, which contain up to 128 sharp, metal-tipped electrodes with a pitch of 200–400 μm, are produced by a combination of micromachining and lithography from thick silicon wafers. Implanted Utah arrays ‘float’ on the surface of the brain and are connected to skull-mounted interface boards by flexible cables. Due to their relatively large area and electrode count, these devices have become crucial components in studies of cortical circuits in non-human primates and are the only neural probes approved by the US Food and Drug Administration (FDA) for chronic use in human patients [25]. As Utah arrays only permit recordings from the topmost 1–3 mm of the cortex with large footprints limiting their utility in small animal models, alternative strategies have been designed for monitoring neural activity at different spatial scales. Michigan probes are composed of lithographically defined patterns of metallic electrodes on thin silicon substrates for depth-defined recordings in subcortical structures [26]. Compatibility of these designs with modern CMOS (complementary metal-oxide semiconductor) processing enables straightforward integration of data acquisition and signal amplification capabilities while allowing for facile back-end connectorization [27, 28]. Both Utah arrays and Michigan probes employ the polymers polyimide and parylene C for insulation. Powered by advances in micro-electromechanical systems (MEMS) fabrication, the past three decades of neural engineering have delivered a multitude of sophisticated probes inspired by Utah and Michigan designs with increased resolution, reduced dimensions and expanded capabilities [29].

The emergence of the fields of neuroprosthetics and brain–machine interfaces, which seek to restore voluntary motor control to paralyzed patients, necessitated the development of high-resolution recording probes. By the late 1990s, decoding algorithms were developed to control robotic joints using rodent and primate brain activity in real time [30, 31]. The surge of scientific and clinical enthusiasm around brain–machine interfaces propelled this

technology into clinical trials in 2004, producing encouraging demonstrations of tetraplegic patients controlling computer cursors [25] and robotic arms [32] with implanted electrode arrays. However, maintaining high SNR recordings from thousands of neurons proved challenging, and biocompatibility and reliability issues often resulted in probe failure only a few weeks after implantation [29, 33, 34].

Materials mismatch

Failure modes of neural probes can be broadly classified into those of engineering and biological origin [33–35] (FIG. 3). The former includes mechanical failure of interconnects between interface boards and implanted probes, degradation of electrical and environmental insulation, and delamination of the different layers constituting the device [29, 35]. To avoid premature failure, microfabricated devices have to be safeguarded from exposure to warm, aqueous and saline environments, and oxidative stress associated with the foreign-body response. Consequently, strategies for packaging and encapsulation have emerged as key aspects of neural-probe design. These include hermetic titanium casings typical of clinical devices, and polyimide, polyurethane, poly(dimethyl sulfoxide) (PDMS), SU-8 and parylene C coatings, which are common in research-grade tools [29].

Foreign-body response.

Neuronal death and formation of glial scars (~100-μm thick) around implanted probes can lead to loss of recorded signals [34, 36]. A subject of several detailed reviews, the glial scar is composed of reactive astrocytes and activated microglia that form dense and electrically inactive tissue along the device surface [34, 36]. A number of factors have been suggested to contribute to this inflammatory response, including: initial tissue damage during device insertion [34, 37]; elastic mismatch between the neural probes and the neural tissue in the context of relative micromotion [35, 38, 39]; disruption of glial networks [40]; chronic breach of the blood-brain barrier [41]; materials neurotoxicity [42]; and chemical mismatch between the implant surface and the cell membranes and extracellular matrix [34].

Although the initial damage due to device insertion may have short-term effects on the recording performance, long-term probe performance is of particular concern to the brain–machine interface community. Introduction of a foreign object with dimensions exceeding 20 μm has been hypothesized to disrupt local communication between glia, which triggers the release of pro-inflammatory cytokines and recruitment of additional activated microglia and reactive astrocytes [34, 40]. The effects of size are challenging to decouple from those associated with elastic mismatch, as smaller device dimensions will also decrease bending stiffness. The elastic mismatch between the neural tissue (kilo- to megapascals) and the implanted probes (1–100 GPa), typically tethered to bone, causes repeated injury to the tissue every time the brain or nerve is displaced relative to the device [35, 38, 39]. This continuous impact has been linked to chronic breach of the blood–brain barrier [41], which activates glia and astrocytes to form a scar around the hemorrhage. In addition to the probe's mechanical properties, surface chemistry and topography may also influence the extent of inflammation [43].

Three decades of neural engineering studies have focused on increasing the reliability and biocompatibility of microfabricated probes through continued miniaturization and addition of coatings to reduce inflammation [44] and modulus mismatch between the probes and neural tissue [45]. However, the innate materials properties of the implants can limit their biocompatibility, which motivated the recent emergence of materials-driven strategies to match the devices' mechanics and geometry to that of neural tissue [46].

Strategies to improve compatibility

Making stiff electronics soft.

Compliant coatings can reduce the apparent elastic mismatch between stiff silicon- or metal-based probes and neural tissue [47]. Hydrogels based on synthetic, biological, or a hybrid of these materials can decrease the surface hardness of the probes, lower electrode impedance and diminish glial scarring. For example, poly(vinyl alcohol) matrix doped with the conductive polymer poly(3,4-ethylenedioxythiophene) (PEDOT) and copolymers of collagen and the organic semiconductor polypyrrole lowered the impedance of lithographically defined metallic electrodes on silicon or glass substrates while improving cell adhesion [48]. Incorporation of neuronal adhesion molecules (for example, L1) [45] or even live cells [49] into the coating may additionally promote local axonal growth.

Polymers have been used as alternative substrates to support microfabricated probes [29, 46] (Fig. 4a). Metal electrodes and interconnects can be lithographically defined or microcontact printed onto polyimide and parylene C substrates. The same polymers are also used for insulation and packaging. Using microcontact printing, integrated multiplexed circuits were integrated with flexible polyimide substrates to map cortical dynamics of epileptic seizures with 500-μm resolution and millisecond precision [50]. Conformal chemical vapor deposition of parylene C onto curved substrates was applied to create complex sheath and hemispherical cavities with internal metal contacts. These flexible neurotrophic electrode cavities were filled with growth factors (for example nerve growth factor and neurotrophin-3) to promote nerve ingrowth and to establish better interfacial contact for improved chronic recording performance [51, 52]. PDMS is also compatible with soft lithography and has been incorporated into devices intended to conform to the dynamic and flexible surfaces of the spinal cord [53] and peripheral nerves [54–56]. Regenerative sieves [56] and nerve-cuff [57] electrodes have also taken advantage of PDMS substrates, which can be rolled into cylindrical shapes tailored to the nerve dimensions to support nerve ingrowth.

To overcome the challenges associated with buckling of flexible probes during insertion into the tissue, polymers that undergo a dramatic reduction in modulus from giga- to megapascal in response to temperature (that is, thermoplastics) [58] and hydration (for example, poly(vinyl acetate)–cellulose composites inspired by sea-cucumber dermis) [59] have been explored as stimuli-responsive substrates for neural interfaces.

The material's bending stiffness (Eq. 1) rather than the Young's modulus determines the tissue interactions for devices tethered to the skull or vertebrae:

$$\frac{F}{d} = \frac{48EI}{L^3} \quad \text{Equation (1)}$$

The bending stiffness is defined as a force needed to achieve a certain deflection. Here F is the force, d is the deflection, E is the Young's modulus, I is the moment of inertia, and L is the length of the device. For a probe with a rectangular cross-section, inputting the expression for the moment of inertia yields:

$$\frac{F}{d} = \frac{4Ewt^3}{L^3} \quad \text{Equation (2)}$$

where w and t are the width and thickness of the device, respectively.

Because the stiffness scales cubically with the material's thickness (Eq. 2), reducing the dimensions of a high-modulus device can dramatically improve its flexibility [60, 61]. This scaling rule has been applied to fabricate compliant microscale wavy surfaces, meshes, serpentines and fibres composed of materials with Young's moduli in the gigapascal range [50, 62–65] (Fig. 4b,c). Contact printed meshes and fractal patterns of silicon and metal ribbons with thicknesses of a few micrometres can act as flexible interconnects between microscale islands bearing recording electrodes as well as other sensors and processing electronics [50, 62]. Out-of-plane buckling of serpentine electrodes deposited onto pre-strained PDMS substrates accommodates stretching by up to ~100 %, which significantly exceeds the strains experienced by peripheral nerves [61] (Fig. 4b). Fibre-drawing can also be applied to reduce the dimensions of metallic electrodes embedded in polymer matrices down to 1–5 μm [65]. Fiber-probes with dimensions of human hair (~80 μm) can integrate 7–10 electrodes with impedance values of ~ 800 kΩ. These probes can record single-unit action potentials and produce negligible impact on the surrounding neural tissue (Fig. 4c). Similarly, carbon fibre can be manually separated [66, 67] or electrospun from carbon nanotube solution [68] to fabricate electrodes 5–10 μm in diameter with impedances of 100 kΩ – 4 MΩ (Fig. 4c). The miniature dimensions of the carbon electrodes also permit isolation of individual action potentials and improved tissue compatibility during chronic implantation [66–68].

Organic and hybrid electronics at neural interface.

Owing to their low moduli, organic conductors are promising platforms for devices intended to interface with biological systems [69] (Fig. 4d). Aromatic small molecules and conjugated polymers have been integrated into neural probes deployed *in vitro* [70]. However, with the exception of PEDOT, the transition of conjugated organics *in vivo* has been impeded by their poor environmental stability [71]. PEDOT mixed with poly(styrene sulfonate) (PEDOT:PSS) is a heavily-doped p-type semiconductor frequently used as a hole-injection and extraction layer in organic light-emitting devices (OLEDs) and photovoltaics, and as a channel in organic field-effect transistors (OFETs) or organic electrochemical transistors [72]. PEDOT:PSS coatings on standard metallic electrodes are known to increase

the SNR and neuronal unit yield [73, 74]. Most recently, flexible PEDOT:PSS organic electrochemical transistors fabricated on 2-μm-thick parylene C substrates were shown to record local field potentials as well as isolated action potentials from the cortical surface [75, 76].

Blends of polymers and conductive micro- and nanoparticles (carbon [77–79], metals [80, 81], conjugated organics [82]) allow for independent control of both the electrode conductivity and bending stiffness [83]. A polymer matrix can be selected for its low modulus, and the conductivity, concentration and geometry of the micro- or nanoscale dopants determine the blend's electronic properties [84] (Fig. 4e,f). Although the majority of nanocomposites are applied as coatings over metallic electrodes, fibre-drawn polyethylene electrodes doped with carbon back were used to record neural activity in the spinal cord of a mouse despite having a high impedance (> 1 MΩ) [78] (Fig. 4e). Doping of PDMS with carbon below the percolation threshold is a promising strategy in designing microstructured piezo-resistive touch sensors [79], and carbon-doped PDMS may eventually be integrated into neural recording probes. More recently, composites of silver nanowires and styrene-butadiene-styrene elastomer patterned into serpentine meshes with elastic moduli of 3–45 kPa (depending on the serpentine curvature) and conductivity ~10^4 S m^{-1} were employed to modulate cardiac firing *in vivo* [80], illustrating the future promise of this material platform for functional interfaces with other electrically active cells (Fig. 4f). As interest in flexible (opto)electronics continues to drive research into conductive polymer composites, a variety of designs initially intended for photovoltaics, OFETs and OLEDs [83, 85] may likely be integrated into future neural interfaces.

Bi-directional neural interfaces

Electrical stimulation.

Although recording electrodes provide insight into the electrophysiological activity within the nervous system, they do not allow for control over its dynamics. Electrical stimulation is clinically approved to treat Parkinson's disease [86], neuropathic pain [87] and is a candidate for alleviating symptoms of major depression [88]. Chemically stable and biocompatible platinum and platinum–iridium electrodes with low impedance (<10 kΩ) are commonly used for electrical stimulation [89]. The relatively modest charge injection capacity (CIC ≈ 0.05–0.15 mC cm^{-2}) of these electrodes can be improved by coatings of iridium oxide to (CIC ≈ 5 mC cm^{-2}) or titanium nitride (CIC ≈ 0.9 mC cm^{-2}). In addition to reducing electrochemical impedance, PEDOT, polypyrrole and their blends with conductive nanomaterials can improve charge injection (CIC ≈ 1–15 mC cm^{-2}) of the stimulating electrodes [89]. The CIC can be further improved by increasing the electrode surface area through texturing. Akin to its deleterious effects on recording electrode performance, glial scarring diminishes the CIC of stimulating electrodes. Hence, strategies aimed to reduce the inflammatory response (for example, flexible substrates and modulus-matching coatings) may simultaneously improve stimulation fidelity [29, 46, 47, 55].

Engineering with optogenetics.

Owing to interference with electrophysiological recording and lack of cellular specificity, the basic mechanisms and therapeutic outcomes of electrical stimulation remain poorly understood [90]. Optogenetics can simultaneously perturb and probe the activity of genetically defined neuronal populations because the optical stimuli are decoupled from electrical recordings [91]. This method relies on genetic introduction of light-sensitive microbial ion channels and pumps, called opsins, into mammalian neurons [92] and other electrically active cells [93–95]. Opsins are membrane proteins harboring the chromophore retinal, which changes conformation in response to visible light to transport ions [96, 97]. These proteins can be used for both excitation and inhibition of neural activity. Excitatory opsins (for example, channelrhodopsin 2 (ChR2)) are cation channels that mediate membrane depolarization to fire action potentials in response to light. Inhibitory opsins are proton or chloride pumps (for example, halorhodopsin, NpHR, and archeorhodopsin, ArCh) that move ions against their concentration gradients to silence neurons through optically driven hyperpolarization [98]. Over the past decade, a palette of opsins with varied absorption spectra and photocycle kinetics have been discovered and engineered [99, 100].

Because visible light needed for opsin activation is scattered and absorbed by neural tissue, optogenetic neuromodulation relies on implanted devices to deliver optical stimuli. To take advantage of simultaneous electrophysiological recording and optogenetic control, early efforts outfitted mature neural recording technologies, such as Utah arrays (Fig. 5a), Michigan probes (Fig. 5b), tetrodes, and microwires (Fig. 5c), with commercially available silica fibres [91, 101–103]. Multimaterial semiconductor processing methods have recently been applied to monolithic integration of LEDs within silicon probes [104, 105]. For example, indium–gallium–nitride (InGaN) quantum wells were epitaxially grown on (111) silicon substrates to create arrays of up to twelve 10 μm × 15 μm blue-emitting micro-LEDs integrated with 32 metallic electrodes (Fig. 5d). Sharing geometry with Michigan probes, these devices enabled depth-defined recording and ChR2-mediated optogenetic stimulation of pyramidal neurons in the rat hippocampus [105]. An innovative alternative to silicon probes is a transparent electrode array composed of n-doped (resistivity, $\rho \approx 0.15\ \Omega\cdot$cm) wide-bandgap semiconductor zinc oxide (ZnO), which permits simultaneous electrical neural recording and delivery of optical stimuli with the same material (Fig. 5e)[106]. Another approach to fabricate transparent probes relies on integration of graphene electrodes and interconnects onto Parylene C substrates. The resulting transparent probes permit optical stimulation through the substrates during neural recording (Fig. 5f) [107].

In addition to bi-directional interface capabilities, biocompatibility should be factored into the design of integrated optoelectronic probes based on semiconductors. As crystalline group III–V and II–VI semiconductors exhibit elastic moduli similar to those of silicon and metals (tens to hundreds of gigapascals), the tools based on these materials are likely to elicit inflammatory responses similar to those observed for mature electrode technologies. Consequently, soft- and hybrid material designs have been explored. Using MEMS processing methods, polymer waveguides composed of SU-8 photoresist were integrated with metal-electrode arrays on polyimide substrates. Although SU-8 can be cytotoxic [42] with limited transmission in the visible spectrum, these initial efforts laid the groundwork

for multifunctional and flexible optoelectronic probes (Fig. 5g)[108]. Contact printing of metallic interconnects, electrodes, blue-emitting GaN micro-LEDs, microscale thermistors and silicon photodiodes onto PDMS produced highly compliant multifunctional probes suitable for optogenetic control of mouse behavior as well as neural recording with minimal damage to surrounding tissue (Fig. 5h)[109].

Alternatively, polycarbonate and cyclic olefin copolymer waveguides and carbon-black-polyethylene composite electrodes can be integrated within all-polymer probes via high-throughput fibre drawing. The flexible fibre probes exhibited bending stiffness of 10 N m^{-1} and enabled simultaneous recording and optical neuromodulation in the mouse brain and spinal cord without triggering significant inflammatory reaction (Fig. 5i) [65, 78].

Delivery of chemical stimuli.

To perturb neural activity via traditional pharmacological [110] or chemogenetic approaches [111], microfluidic channels can be integrated into neural probes to deliver chemical and biological agents into the nervous system. Optogenetic stimulation augmented by delivery of a neuromodulator (for example, a synaptic blocker) may reduce the ambiguity in optical cell-type identification experiments, where opsin expression is used to mark a particular neuronal population [103, 104]. Furthermore, microfluidic channels permit injection of viral vectors needed for genetic experiments when transgenic animal models are not available [112]. Glial scar formation within the probe vicinity may block the microfluidic channels or change the diffusivity of the compounds of interest. Although integration of microfluidic features into flexible MEMS-processed [51, 108], microcontact printed [112] and fibre-drawn neural probes [65] increases the size of the device, these probes are significantly smaller than devices assembled from bulky cannulas, silica optical fibers and metallic electrodes, and hence may reduce the foreign-body response (Fig. 5g–i).

Wireless transmission.

Backend connections scale proportionally with the addition of functional features integrated into the implants. The increased device complexity and weight can affect the behavior of the experimental subjects, especially smaller animal models. Wireless power and data transmission can eliminate the need for multiple tethers and headstages [113], but may result in significant heat dissipation within the implanted hardware owing to high data rates and power draws. Furthermore, the physical dimensions of radiofrequency antennas may not be compatible with implantation into small rodents unless designed for a limited transmission range.

Recent implants powered by radiofrequency antennas enable wireless operation of semiconductor micro-LEDs to optically drive behaviour in mice expressing ChR2 in the brain, spinal cord and peripheral nerves [114, 115]. Both direct transmission [115] and evanescent coupling through the animal body [114] has been explored as a means to deliver the necessary power. The former relied on microcontact serpentine antennas with areas of ~3×3 mm^2, and the latter required a specialized radiofrequency cavity positioned directly underneath a behavioural enclosure. For applications requiring additional functionality, such

as multiple optical sources or microfluidic drug delivery, larger antennas mounted on the skull were used [112].

Independently operating wireless microcircuits tens to hundreds of micrometres in size, called ‘neural dust’ motes, have been proposed as an alternative technology to traditional probes [116]. Initial millimeter-scale prototypes have been fabricated and are capable of recording and electrically evoking activity in peripheral nerves [117]. However, further miniaturization poses challenges to device placement and stability within the nervous system.

From microprobes to nanotransducers

Micro- and nanostructured electrodes permit intracellular recordings and modulation of sub-threshold events at finer temporal resolution and longer duration than conventional patch-clamp electrophysiology. Micrometre-sized gold mushrooms, functionalized with RGD peptides to promote cell adhesion, provided intracellular-like recordings of action potentials as well as subthreshold synaptic activity for days *in vitro* [118, 119] (Fig. 6a). However, translation of this technology *in vivo* is challenging because of its reliance on intimate contact between high impedance (~30 MΩ) mushroom electrodes and neurons. Monocrystalline gold nanowires ~100 nm in diameter also exhibit high impedances (~5 MΩ), but were found to be effective for acute recordings of single unit activity in the CA1 region of the mouse hippocampus [120]. Silicon-nanowire and gold-nanopillar electrodes were used for intracellular recordings following localized membrane electroporation, although intracellular access was lost within minutes owing to membrane resealing [121, 122]. To prolong intracellular access, hollow nanotube electrodes that form tight junctions with the cell membrane were synthesized [123]. Stealthy probes with amphiphilic coatings that mimic the chemical structure of cell membranes may also provide passive access to the cytosol through spontaneous fusion [124] (Fig. 6b).

In addition to capacitive voltage recordings, modulation of the gate voltage of semiconductor-nanowire FETs by controlling the local ion flux can also be used for *in vitro* extracellular neural recording (Fig. 6c) [125, 126]. The same study found that nanowire FET arrays are sensitive enough to capture the propagation of action potentials down individual axons [125]. To achieve high-resolution intracellular recordings in three dimensions, FET extension from planar substrates was enabled by the synthesis of kinked nanowires [127, 128]. Although electrode miniaturization and morphological control are promising strategies for long-term intracellular recording, the challenges in device connectorization and implantation currently limit these technologies primarily to *in vitro* models.

To harness the resolution of nanoscale electronics *in vivo*, macroporous meshes have been developed that have mechanical properties similar to neural tissue [129] [130]. These metal meshes supported by SU-8 substrates served to connect nanowire FETs and platinum nanoelectrodes to backend electronics and could be injected into the brain. These devices provided chronic single-unit recording while also acting as ‘neurophilic’ scaffolds promoting neuronal migration [129–131].

Despite the miniaturization and increased flexibility of neural probes, a device that eliminates connectorized hardware and tissue damage while communicating with the nervous system over arbitrarily long timescales remains to be demonstrated. By contrast, contactless stimuli coupled to nanoparticle transducers may facilitate localized readout or perturbation of neural activity at single-protein resolution [132]. Advances in synthetic methods have delivered nanomaterials with tunable size, shape and composition. Furthermore these nanomaterials can be decorated with functional groups for cell-specific targeting and improved biocompatibility [133, 134].

Contactless communication

Optical, acoustic and magnetic stimuli offer application-specific advantages for neural stimulation and recording [135] (Fig. 7). While optical stimulation and imaging approaches, such as infrared light [136], genetically encoded opsins [137, 138], and calcium and voltage indicators [139], offer superior spatial and temporal resolution, they are limited to tissue penetration depths of less than 1 mm owing to absorbance and scattering. Even three-photon excitation with a 1675-nm laser can only penetrate to a depth of 1.5 mm into brain structures [140].

Acoustic waves can extend the penetration depth by one to two orders of magnitude in a frequency-dependent manner [141, 142]. Transcranial focused ultrasound at frequencies below 0.65 MHz and amplitude of 0.12 MPa was shown to modulate activity 3-cm deep in the human somatosensory cortex [143]. Although ultrasound signals with lower frequencies offer deeper tissue penetration without significant attenuation, the resolution is proportional to wavelength, which yields modulation volumes greater than 1 mm^3 [142]. Functional ultrasound can map blood vessels in the neural tissue based on the characteristic Doppler frequency associated with the movement of blood cells through the imaging pixels [144]. Because neural activity within a given region is correlated with increased blood flow, this approach permits non-invasive and indirect measurement of neural dynamics. Without a contrast agent, a 15-MHz functional ultrasound probe enables hemodynamic imaging across the entire rat brain with a resolution 100 μm × 100 μm × 200 μm in 200 ms [144]. Although this method does not rely on implanted conduits, it necessitates mounting the functional ultrasound probe over an aqueous cranial window to avoid scattering from the skull.

Magnetic fields are the only modality that can access arbitrarily deep tissues with little attenuation owing to the low magnetic susceptibility of biological matter [145, 146]. Magnetic fields with frequencies below 1 kHz and amplitudes above 1 T can inductively evoke ionic currents to non-invasively modulate brain activity through the skull [147]. However, transcranial magnetic stimulation is limited by the coil geometry [148], and clinical applications are constrained primarily to cortical structures with centimetre spatial resolution. Functional magnetic resonance imaging (fMRI) exploits the differences between the magnetic properties of oxygenated and deoxygenated hemoglobin to measure a local increase in blood flow that accompanies neural activity [149]. Although non-invasive, this method has limited spatial and temporal resolution of ~0.5 mm × 0.5 mm voxel area and a sampling rate of less than 2 Hz.

Nanoscale transducers that convert optical, acoustic and magnetic stimuli into biological cues may extend the signal penetration depth and improve the spatial and temporal resolution of noninvasive neural recording and modulation approaches [150] (Fig. 8). Semiconductor quantum dots, gold nanoparticles and upconversion NPs can respectively convert light into voltage, heat, or light of a different wavelength (Fig. 8a–c). The deformation induced by ultrasound can be amplified by microbubbles [151] or be converted into electric fields by piezoelectric materials (Fig. 8d–e). Magnetic nanoparticles can cluster [152], transduce force [153] and apply torque in stationary field gradients, or dissipate heat through hysteresis in alternating magnetic fields [154] (Fig. 8g–i). Interfacing magnetostrictive and ferroelectric materials enables conversion of a magnetic field into an electrical potential [155]. This list, by no means exhaustive, represents a diverse and relatively unexplored materials toolkit for potential next-generation neurotechnologies [150].

Neural interrogation with nanomaterials

Optical nanomaterials.

Optically active inorganic nanomaterials have been explored as non-genetic tools for precise spatial and temporal control and recording of neural activity (Fig. 8a–c). Optical excitation of quantum dots embedded within the cell membrane can, in principle, generate sufficient localized electric fields to trigger action-potential firing [156] (Fig. 8a). However, to date, only quantum-dot films have been demonstrated to excite neurons upon light exposure [156, 157]. Field-induced photoluminescence quenching in quantum dots owing to ionization or the quantum-confined Stark effect may enable their use as voltage sensors [158, 159]. Technical challenges of using these materials *in vivo* include the cytotoxicity of quantum dots, which are composed primarily of heavy metals (Cd, Pb), and the difficulty in embedding them into the cell membrane [160]. Gold nanoparticles are significantly more biocompatible and can couple to light through surface plasmon resonance [161]. Plasmonic heating in gold nanoparticles can induce neural inhibition under constant illumination [162] or neural excitation with pulsed laser light at frequencies up to 40 Hz [163] (Fig. 8b). This photothermal approach allows operation at optical power densities lower than those needed to excite ChR2 while offering sub-cellular resolution [163–165]. Because surface plasmons are sensitive to local electric fields, they may be developed into voltage sensors [166], albeit with narrower dynamic range than quantum dots [159, 167]. Nanodiamonds harbouring nitrogen-vacancy colour centres with photoluminescence sensitive to temperature [168], electric and magnetic fields are emerging as biocompatible candidates for optical imaging of cellular activity [169, 170].

Upconversion nanoparticles absorb near-infrared light and emit shorter wavelengths via multiphoton processes (Fig. 8c). This effect can extend the penetration depth of optical stimuli, because tissue scattering is reduced in the near-infrared-light region [171]. For example, lanthanide-doped upconversion nanoparticles absorbing 980-nm light were used to control isomerization of the blue-light-sensitive LOV-domain to drive gene transcription [172].

Mechanoresponsive nanomaterials.

To improve the resolution of transcranial ultrasound stimulation while maintaining penetration depths greater than 1 cm [143], mechanoresponsive nanomaterials can be used to control targeted neurons by local amplification of low-intensity ultrasound. Perfluorohexane microbubbles undergoing physical deformation upon exposure to ultrasound (0.2–1 MPa, 2.55 MHz) have been shown to affect the behaviour of *C. elegans* [173] (Fig. 8d). This effect was linked to the mechanosensitive ion channel TRPV4 expressed in sensory neurons, which transduce the localized deformation during microbubble cavitation into cation influx and firing of action potentials [173]. To eliminate the reliance on mechanosensitive channels, piezoelectric barium titanate ($BaTiO_3$) nanoparticles have been engineered to convert ultrasound into an electric field [174] (Fig. 8e). Ca^{2+} influx in response to ultrasound was observed in neuron-like PC12 cells in close proximity to micrometre-sized $BaTiO_3$ aggregates [174]. These early examples demonstrate the potential of acoustic sensitizers to evoke neural activity when placed near the cell membrane. Future work in primary neurons and animal models should assess the efficacy of this neuromodulation technology. In addition to their use in neural stimulation, microbubbles and genetically encoded nano-vesicles (Fig. 8e, f) can improve the resolution of functional ultrasound imaging by two orders of magnitude, achieving hemodynamic brain mapping with a pixel size of 8 μm × 10 μm in a given illuminated plane [151].

Magnetic nanomaterials.

Magnetic nanoparticles (MNPs) can transduce a broad range of stimuli in the presence of magnetic fields and offer a versatile toolkit for contactless perturbation of cellular function (Fig. 8g–i). In a static field gradient, MNPs transduce force to actuate the opening of mechanosensitive ion channels or cluster to switch on aggregation-dependent cell pathways [175]. Relatively large forces in the piconewton range are required to trigger mechanosensitive ion channels [176], which necessitates the use of high field gradients (>5 T m^{-1}) and particles with large magnetic moments to evoke a cellular event [153, 175, 177, 178]. By contrast, forces of only a few femtonewton can drive lateral association of receptors embedded in lipid membranes (Fig. 8g). This mechanism was exploited to induce apoptosis through clustering of MNPs linked to death receptor 4 (DR4) in an applied field of 0.2 T [152]. Because the MNPs' magnetic moment and targeting moieties can be varied independently via their size, composition, and surface functionalization, a variety of mechanical and chemical cues can be delivered with high spatial and temporal precision [179].

Alternating magnetic fields (AMFs) can also be applied to control cellular function. For example, micrometre-sized magnetizable ferrite-doped beads and permalloy discs can disrupt the cytoskeleton or cell membrane by exerting torque in a slowly varying field (10–50 Hz) [180, 181] (Fig. 8h). AMFs with frequencies up to 5 kHz coupled to superparamagnetic zinc-doped ferrite ($Zn_{0.4}Fe_{2.6}O4$) nanocubes can induce deflection and Ca^{2+} influx in mechanosensitive inner-ear hair cells [153] (Fig. 8h). In AMFs with low radiofrequencies (100 kHz–1 MHz) and amplitudes (10–100 mT), chemically inert ferrite MNPs ($Me_xFe_{3-x}O_4$, Me = Fe, Co, Mn, Zn) can undergo hysteresis and dissipate heat [182] (Fig. 8i). This phenomenon, which arises from irreversible work done during a

magnetization cycle, has been investigated as a potential cancer treatment for nearly 5 decades. More recently, magnetic hyperthermia was applied to remote control of action-potential firing [183, 184] and gene transcription [185]. AMF-driven heat dissipation by MNPs can trigger the opening of the heat-sensitive transient potential receptor vanilloid channel 1 (TRPV1) leading to Ca^{2+} influx and action-potential firing in neurons [183, 184]. Magnetothermal neuromodulation can be formulated as a simple injection into a deep brain structure sensitized to heat via cell-specific TRPV1 expression to enable chronic stimulation [183].

Multiferroic composite nanoparticles consisting of magnetostrictive and piezoelectric phases enable remote magnetic control of the nanoparticle's dipole moment. Magnetoelectric nanomaterials composed of magnetostrictive $CoFe_2O_4$ nanoparticles coated with piezoelectric $BaTiO_3$ shells can release electrostatically adsorbed drugs [186], and may be employed as transducers for wireless magnetoelectric neuromodulation [187].

MNPs can also be used as MRI (magnetic resonance imaging) probes of neural activity. At physiological temperatures, isolated superparamagnetic nanoparticles on average have zero magnetic moment. When clustered, the dipole–dipole interactions between the nanoparticles impart non-zero net magnetic moment onto the aggregates [188]. The change in magnetic moment can be recorded by MRI as a change in contrast, allowing for detection of events other than hemodynamics [189]. For example, MNPs conjugated to the Ca^{2+}-binding protein calmodulin enable MRI measurement of Ca^{2+} concentration [190]. Although diffusion kinetics currently limits the efficacy of this method *in vivo* [191], improvement in clustering schemes may significantly enhance sensor sensitivity and the dynamic range [192]. With further refinement, these nanoparticle sensors may offer higher signal contrast at lower concentrations than current small molecule agents used for real-time MRI monitoring of neurotransmitter levels in the brain [193].

Prospects and challenges

Emerging applications of nanomaterials at the neural interface demonstrate the possibility of contactless neuromodulation and recording without fixed hardware and transgenes. Further gain in function can be envisioned through combinatorial strategies involving multiple nanomaterials and external stimuli. For example, independent neuromodulation of different cell populations may be possible by tailoring the nanomaterial properties, such as using MNPs that selectively dissipate heat in distinct AMF conditions or plasmonic gold nanorods that absorb light at different wavelengths [194, 195]. Materials optimization for a specific transduction mechanism can reduce stimulation latency [196] or enhance reporter sensitivity [159]. Finally, integration of probes that transduce orthogonal stimuli may further expand the experimental palette.

The delivery of nanomaterials *in vivo* is perhaps a bigger design challenge than optimizing the nanomaterials' intrinsic properties [197]. The nanoparticles' ability to target the site of interest and its residential lifetime at the neural interface depends on a number of factors including nanoparticles' surface chemistry, size, shape, composition and concentration. Although antibody conjugation to NPs affords specificity *in vitro*, non-specific protein

adsorption and poor colloidal stability may impede this targeting approach *in vivo* [198, 199]. Difficulty in traversing the blood–brain barrier [197] and transient lifetime on the cell membrane [200] render cell-specific and chronic neural interfaces with nanoparticles technically challenging. Non-surgical strategies to deliver nanoparticles to a particular brain region include functional-ultrasound-assisted temporary breach of the blood–brain barrier [201] and, for MNPs, spatial localization with magnetic-field gradients [202]. Improvement of these delivery methods may eventually allow nanoparticles to target a particular neural circuit by periodic intravenous or oral administration to overcome the transient nature of the nanomaterial–neuron interface. When invasive delivery is acceptable, nanoparticles can be directly injected into the region of interest. Amino-functionalized MNPs can persist up to a year in the human brain [203]. In the peripheral nervous system, nanoparticles can be injected into a targeted nerve encapsulated within a scaffolding material that delays nanoparticle clearance [204–206].

Biogenic nanomaterials can circumvent the difficulties in cell-specific nanoparticle targeting and their clearance through constant expression of the relevant protein complexes from the integrated transgenes. Gas-filled vesicles can be genetically encoded and engineered to improve temporal and spatial resolution of functional ultrasound imaging [207]. Magnetogenetic excitation and inhibition of neural activity in mice was recently reported with ion channels fused to ferritin [208, 209], a protein which can mineralize iron into weakly paramagnetic ferrihydrite [210]. Unlike synthetic MNPs composed of ferrimagnetic iron oxide and its alloys, ferritin possesses negligible magnetic moment, and the biophysical origins of the observed physiological response to applied magnetic fields thus remain unclear [211]. Magnetotactic bacteria are known to produce magnetite nanoparticles, which have significantly higher magnetic moments than ferritin [212]. However, transferring their genetic machinery into mammalian cells requires further optimization [213].

Conclusion and outlook

Multifunctional devices capable of forming intimate interfaces with neurons without provoking a severe foreign-body response would provide detailed maps of neural activity and serve as neuroprosthetic links with electronic circuits. Although nano- and microfabricated neural probes offer unprecedented resolution and temporal precision, the mismatch in mechanical and chemical properties of metals, oxides and semiconductors with neural tissue has frequently lead to the probe failure with time.

Fueled by advances in materials synthesis and flexible electronics, over the past decade, materials-centric designs have steadily reduced the foreign-body response at the brain–machine interface. Concomitantly, the development of opto- and chemogenetic tools has brought new opportunities for neuroscientists and inspired engineers to integrate optical and microfluidic features into neural probes. However, the reliance on fixed hardware for signal transduction, still limits the number of neurons that can be independently addressed across the nervous system.

Synthetic nanomaterials, with their diverse and tunable properties, can transduce optical, acoustic and magnetic stimuli into biological signals and vice versa. Although targeting of

nanomaterials into specific locations of the nervous system presents a formidable challenge, the potential payoff is the ability to remotely control and record the activity of billions of neurons. Genetically encoded reporters and mediators of neural activity have improved our understanding of brain and nerve function, and have contributed insight into future therapies for neurological disorders. Their clinical translation, however, remains uncertain, and will require new technologies that will likely operate at the nanoscale to conform to the complexity of the nervous system.

Acknowledgements

PA is supported by the National Science Foundation (NSF) through CAREER Award, Center for Materials Science and Engineering, and Center for Sensorimotor Neural Engineering, National Institutes for Neurological Disorders and Stroke, the Defense Advanced Research Projects Agency, Dresselhaus Fund Award, and the Bose Research Grant.

References

1. Dorsey ER, et al., Projected number of people with Parkinson disease in the most populous nations, 2005 through 2030. Neurology, 2007 68(5): p. 384–6. [PubMed: 17082464]
2. Adelman G, Rane SG, and Villa KF, The cost burden of multiple sclerosis in the United States: a systematic review of the literature. J Med Econ, 2013 16(5): p. 639–47. [PubMed: 23425293]
3. Greenberg PE, et al., The economic burden of depression in the United States: how did it change between 1990 and 2000? J Clin Psychiatry, 2003 64(12): p. 1465–75. [PubMed: 14728109]
4. Mathers CD and Loncar D, Projections of Global Mortality and Burden of Disease from 2002 to 2030. PLoS Med, 2006 3(11): p. e442. [PubMed: 17132052]
5. Tracey KJ, Reflex control of immunity. Nat Rev Immunol, 2009 9(6): p. 418–428. [PubMed: 19461672]
6. Kandel E, Schwartz J, Jessell T, Principles of Neural Science. 4th edition ed. 2000: McGraw-Hill Medical.
7. Azevedo FA, et al., Equal numbers of neuronal and nonneuronal cells make the human brain an isometrically scaled-up primate brain. J Comp Neurol, 2009 513(5): p. 532–41. [PubMed: 19226510]
8. Haydon PG, Glia: listening and talking to the synapse. Nat Rev Neurosci, 2001 2(3): p. 185–193. [PubMed: 11256079]
9. Barres BA, The Mystery and Magic of Glia: A Perspective on Their Roles in Health and Disease. Neuron, 2008 60(3): p. 430–440. [PubMed: 18995817]
10. Pakkenberg B, et al., Aging and the human neocortex. Experimental Gerontology, 2003 38(1–2): p. 95–99. [PubMed: 12543266]
11. Wemmie JA, Taugher RJ, and Kreple CJ, Acid-sensing ion channels in pain and disease. Nat Rev Neurosci, 2013 14(7): p. 461–471. [PubMed: 23783197]
12. Patapoutian A, et al., ThermoTRP channels and beyond: mechanisms of temperature sensation. Nat Rev Neurosci, 2003 4(7): p. 529–539. [PubMed: 12838328]
13. Jordt S-E, McKemy DD, and Julius D, Lessons from peppers and peppermint: the molecular logic of thermosensation. Current Opinion in Neurobiology, 2003 13(4): p. 487–492. [PubMed: 12965298]
14. Delmas P, Hao J, and Rodat-Despoix L, Molecular mechanisms of mechanotransduction in mammalian sensory neurons. Nat Rev Neurosci, 2011 12(3): p. 139–153. [PubMed: 21304548]
15. Strumwasser F, Long-Term Recording from Single Neurons in Brain of Unrestrained Mammals. Science, 1958 127(3296): p. 469–470. [PubMed: 13529005]
16. Sakmann B, Neher E, Patch clamp techniques for studying ionic channels in excitable membranes. Annual Review of Physiology, 1984 46: p. 455–472.

17. Campbell PK, Jones KE, Huber RJ, Horch KW, Normann RA, A silicon-based, three-dimensional neural interface: manufacturing processes for an intracortical electrode array. IEEE Transactions in Biomedical Engineering, 1991 38: p. 758–768.
18. Drake KL, Wise KD, Farraye J, Anderson DJ, BeMent SL, Performance of planar multisite microprobes in recording extracellular single-unit intracortical activity. IEEE Transactions on Biomedical Engineering, 1988 35(9): p. 719–732. [PubMed: 3169824]
19. McNaughton BL, O'Keefe J, Barnes CA, The stereotrode: a new technique for simultaneous isolation of several single units in the central nervous system from multiple unit records. Journal of Neuroscience Methods, 1983 8: p. 391–397. [PubMed: 6621101]
20. Gray CM, Maldonado PE, Wilson M, McNaughton B, Tetrodes markedly improve the reliability and yield of multiple single-unit isolation from multi-unit recordings in cat striate cortex. Journal of Neuroscience Methods, 1995 63: p. 43–54. [PubMed: 8788047]
21. Aronov D, Andalman AS, and Fee MS, A specialized forebrain circuit for vocal babbling in the juvenile songbird. Science, 2008 320(5876): p. 630–4. [PubMed: 18451295]
22. Herry C, Ciocchi S, Senn V, Demmou L, Muller C, Lüthi A, Switching on and off fear by distinct neuronal circuits. Nature, 2008 454(7204): p. 600–6. [PubMed: 18615015]
23. Wilson MA and McNaughton BL, Reactivation of hippocampal ensemble memories during sleep. Science, 1994 265(5172): p. 676–9. [PubMed: 8036517]
24. Bartels J, Andreasen D, Ehirim P, Mao H, Seibert S, Wright EJ, Kennedy P, Neurotrophic electrode: method of assembly and implantation into human motor speech cortex. Journal of Neuroscience Methods, 2008 174(2): p. 168–76. [PubMed: 18672003]
25. Hochberg LR, et al., Neuronal ensemble control of prosthetic devices by a human with tetraplegia. Nature, 2006 442(7099): p. 164–171. [PubMed: 16838014]
26. Buzsaki G, et al., High-frequency network oscillation in the hippocampus. Science, 1992 256(5059): p. 1025–7. [PubMed: 1589772]
27. Yazicioglu F, et al., Ultra-high-density in-vivo neural probes. Conf Proc IEEE Eng Med Biol Soc, 2014 2014: p. 2032–5. [PubMed: 25570383]
28. Wise KD, Silicon microsystems for neuroscience and neural prostheses. IEEE Eng Med Biol Mag, 2005 24(5): p. 22–9.
29. Scholten K and Meng E, Materials for microfabricated implantable devices: a review. Lab on a Chip, 2015 15(22): p. 4256–4272. [PubMed: 26400550]
30. Nicolelis MAL, Brain-machine interfaces to restore motor function and probe neural circuits. Nat Rev Neurosci, 2003 4(5): p. 417–422. [PubMed: 12728268]
31. Donoghue JP, Connecting cortex to machines: recent advances in brain interfaces. Nature neuroscience, 2002.
32. Hochberg LR, Bacher D, Jarosiewicz B, Masse NY, Simeral JD, Vogel J, Haddadin S, Liu J, Cash SS, van der Smagt P, Donoghue JP, Reach and grasp by people with tetraplegia using a neurally controlled robotic arm. Nature, 2012 485(7398): p. 372–375. [PubMed: 22596161]
33. Ward MP, Rajdev P, Ellison C, Irazoqui PP, Toward a comparison of microelectrodes for acute and chronic recordings. Brain Research, 2009 1282(0): p. 183–200. [PubMed: 19486899]
34. Polikov VS, Tresco PA, Reichert WM, Response of brain tissue to chronically implanted neural electrodes. Journal of Neuroscience Methods, 2005 148(1): p. 1–18. [PubMed: 16198003]
35. James CB, et al., Failure mode analysis of silicon-based intracortical microelectrode arrays in non-human primates. Journal of Neural Engineering, 2013 10(6): p. 066014. [PubMed: 24216311]
36. Kozai TDY, et al., Brain Tissue Responses to Neural Implants Impact Signal Sensitivity and Intervention Strategies. ACS Chemical Neuroscience, 2015 6(1): p. 48–67. [PubMed: 25546652]
37. Ward MP, Rajdev P, Ellison C, Irazoqui PP, Toward a comparison of microelectrodes for acute and chronic recordings. Brain Research, 2009 1282: p. 183–200. [PubMed: 19486899]
38. Lee H, Bellamkonda RV, Sun W, Levenston ME, Biomechanical analysis of silicon microelectrode-induced strain in the brain. Journal of Neural Engineering, 2005 2: p. 81–89. [PubMed: 16317231]
39. Lind G, Linsmeier CE, Schouenborg J, The density difference between tissue and neural probes is a key factor for glial scarring. Sci Rep, 2013 3: p. 2942. [PubMed: 24127004]

40. Szarowski DH, Andersen MD, Retterer S, Spence AJ, Isaacson M, Craighead HG, Turner JN, Shain W, Brain responses to micro-machined silicon devices. Brain Research, 2003 983(1–2): p. 23–35. [PubMed: 12914963]
41. Saxena T, Karumbaiah L, Gaupp EA, Patkar R, Patil K, Betancur M, Stanley GB, Bellamkonda RV, The impact of chronic blood-brain barrier breach on intracortical electrode function. Biomaterials, 2013 34(20): p. 4703–13. [PubMed: 23562053]
42. Kotzar G, et al., Evaluation of MEMS materials of construction for implantable medical devices. Biomaterials, 2002 23(13): p. 2737–2750. [PubMed: 12059024]
43. Chapman CAR, et al., Nanoporous Gold as a Neural Interface Coating: Effects of Topography, Surface Chemistry, and Feature Size. ACS Applied Materials & Interfaces, 2015 7(13): p. 7093–7100. [PubMed: 25706691]
44. Zhong Y, Bellamkonda RV, Dexamethasone-coated neural probes elicit attenuated inflammatory response and neuronal loss compared to uncoated neural probes. Brain Res, 2007 1148: p. 15–27. [PubMed: 17376408]
45. Azemi E, et al., Surface immobilization of neural adhesion molecule L1 for improving the biocompatibility of chronic neural probes: In vitro characterization. Acta Biomaterialia, 2008 4(5): p. 1208–1217. [PubMed: 18420473]
46. Jeong J-W, Shin G, Park SI, Yu KJ, Xu L, Rogers JA, Soft Materials in Neuroengineering for Hard Problems in Neuroscience. Neuron, 2015 86(1): p. 175–186. [PubMed: 25856493]
47. Aregueta-Robles UA, et al., Organic electrode coatings for next-generation neural interfaces. Frontiers in Neuroengineering, 2014 7.
48. Kim D-H, Wiler JA, Anderson DJ, Kipke DR, Martin DC, Conducting polymers on hydrogel-coated neural electrode provide sensitive neural recordings in auditory cortex. Acta Biomaterialia, 2010 6(1): p. 57–62. [PubMed: 19651250]
49. Green RA, Lovell NH, and Poole-Warren LA, Cell attachment functionality of bioactive conducting polymers for neural interfaces. Biomaterials, 2009 30(22): p. 3637–3644. [PubMed: 19375160]
50. Viventi J, Kim DH, Vigeland L, Frechette ES, Blanco JA, Kim YS, Avrin AE, Tiruvadi VR, Hwang SW, Vanleer AC, Wulsin DF, Davis K, Gelber CE, Palmer L, Van der Spiegel J, Wu J, Xiao J, Huang Y, Contreras D, Rogers JA, Litt B, Flexible, foldable, actively multiplexed, high-density electrode array for mapping brain activity in vivo. Nature neuroscience, 2011 14: p. 1599–1605. [PubMed: 22081157]
51. Kim BJ, Kuo JT, Hara SA, Lee CD, Yu L, Gutierrez CA, Hoang TQ, Pikov V, Meng E, 3D Parylene sheath neural probe for chronic recordings. Journal of neural engineering, 2013 10(4): p. 045002. [PubMed: 23723130]
52. Tooker A, Meng E, Erickson J, Tai YC, Pine J Development of biocompatible parylene neurocages. in Engineering in Medicine and Biology Society, 2004. IEMBS '04. 26th Annual International Conference of the IEEE 2004.
53. Minev IR, et al., Electronic dura mater for long-term multimodal neural interfaces. Science, 2015 347(6218): p. 159–163. [PubMed: 25574019]
54. Delivopoulos E, et al., Concurrent recordings of bladder afferents from multiple nerves using a microfabricated PDMS microchannel electrode array. Lab on a chip, 2012 12(14): p. 2540–51. [PubMed: 22569953]
55. Lacour SP, Benmerah S, Tarte E, FitzGerald J, Serra J, McMahon S, Fawcett J, Graudejus O, Yu Z, Morrison B 3rd, Flexible and stretchable micro-electrodes for in vitro and in vivo neural interfaces. Medical & biological engineering & computing, 2010 48(10): p. 945–54. [PubMed: 20535574]
56. Srinivasan A, et al., Microchannel-based regenerative scaffold for chronic peripheral nerve interfacing in amputees. Biomaterials, 2015 41: p. 151–165. [PubMed: 25522974]
57. FitzGerald JJ, Lago N, Benmerah S, Serra J, Watling CP, Cameron RE, Tarte E, Lacour SP, McMahon SB, Fawcett JW, A regenerative microchannel neural interface for recording from and stimulating peripheral axons in vivo. Journal of neural engineering, 2012 9(1): p. 016010. [PubMed: 22258138]
58. Ware T, et al., Fabrication of Responsive, Softening Neural Interfaces. Advanced Functional Materials, 2012 22(16): p. 3470–3479.

59. Capadona JR, Shanmuganathan K, Tyler DJ, Rowan SJ, Weder C, Stimuli-responsive polymer nanocomposites inspired by the sea cucumber dermis. Science, 2008 319(5868): p. 1370–4. [PubMed: 18323449]
60. Kim D-H, et al., Flexible and Stretchable Electronics for Biointegrated Devices. Annual Review of Biomedical Engineering, 2012 14(1): p. 113–128.
61. Rogers JA, Someya T, and Huang Y, Materials and Mechanics for Stretchable Electronics. Science, 2010 327(5973): p. 1603–1607. [PubMed: 20339064]
62. Kim DH, Lu N, Ma R, Kim YS, Kim RH, Wang S, Wu J, Won SM, Tao H, Islam A, Yu KJ, Kim TI, Chowdhury R, Ying M, Xu L, Li M, Chung HJ, Keum H, McCormick M, Liu P, Zhang YW, Omenetto FG, Huang Y, Coleman T, Rogers JA, Epidermal electronics. Science, 2011 333: p. 838–343. [PubMed: 21836009]
63. Kim R-H, et al., Waterproof AlInGaP optoelectronics on stretchable substrates with applications in biomedicine and robotics. Nat Mater, 2010 9(11): p. 929–937. [PubMed: 20953185]
64. Fan JA, et al., Fractal design concepts for stretchable electronics. Nat Commun, 2014 5.
65. Canales A, Jia X, Froriep UP, Koppes RA, Tringides CM, Selvidge J, Hou C, Wei L, Fink Y, Anikeeva P, Multifunctional fibers for simultaneous optical, electrical and chemical interrogation of neural circuits in vivo. Nature Biotechnology, 2015 33(3): p. 277–284.
66. Kozai TD, Langhals NB, Patel PR, Deng X, Zhang H, Smith KL, Lahann J, Kotov NA, Kipke DR, Ultrasmall implantable composite microelectrodes with bioactive surfaces for chronic neural interfaces. Nature Materials, 2012 11(12): p. 1065–73. [PubMed: 23142839]
67. Guitchounts G, Markowitz JE, Liberti WA, Gardner TJ, A carbon-fiber electrode array for long-term neural recording. Journal of Neural Engineering, 2013 10(4): p. 046016. [PubMed: 23860226]
68. Vitale F, et al., Neural Stimulation and Recording with Bidirectional, Soft Carbon Nanotube Fiber Microelectrodes. ACS Nano, 2015.
69. Malliaras GG, Organic bioelectronics: A new era for organic electronics. Biochimica et Biophysica Acta (BBA) - General Subjects, 2013 1830(9): p. 4286–4287. [PubMed: 23079584]
70. Benfenati V, et al., A transparent organic transistor structure for bidirectional stimulation and recording of primary neurons. Nat Mater, 2013 12(7): p. 672–680. [PubMed: 23644524]
71. Kawano K, et al., Degradation of organic solar cells due to air exposure. Solar Energy Materials and Solar Cells, 2006 90(20): p. 3520–3530.
72. Elschner Andreas, S.K., Lovenich Wilfried, Merker Udo, Reuter Knud, PEDOT, Principles and Applications of an Intrinsically Conductive Polymer 2010: CRC Press.
73. Kip AL, et al., Chronic neural recordings using silicon microelectrode arrays electrochemically deposited with a poly(3,4-ethylenedioxythiophene) (PEDOT) film. Journal of Neural Engineering, 2006 3(1): p. 59. [PubMed: 16510943]
74. Ludwig KA, Langhals NB, Joseph MD, Richardson-Burns SM, Hendricks JL, Kipke DR, Poly(3,4-ethylenedioxythiophene) (PEDOT) polymer coatings facilitate smaller neural recording electrodes. Journal of Neural Engineering, 2011 8.
75. Khodagholy D, et al., In vivo recordings of brain activity using organic transistors. Nat Commun, 2013 4: p. 1575. [PubMed: 23481383]
76. Khodagholy D, et al., NeuroGrid: recording action potentials from the surface of the brain. Nat Neurosci, 2015 18(2): p. 310–315. [PubMed: 25531570]
77. Castagnola E, et al., Biologically Compatible Neural Interface To Safely Couple Nanocoated Electrodes to the Surface of the Brain. ACS Nano, 2013 7(5): p. 3887–3895. [PubMed: 23590691]
78. Lu C, Froriep UP, Canales A, Koppes RA, Caggiano V, Selvidge J, Bizzi E, Anikeeva P, Polymer fiber probes enable optical control of spinal cord and muscle function in vivo. Advanced Functional Materials, 2014 24(42): p. 6594–6600.
79. Tee BC-K, et al., A skin-inspired organic digital mechanoreceptor. Science, 2015 350(6258): p. 313–316. [PubMed: 26472906]
80. Park J, et al., Electromechanical cardioplasty using a wrapped elasto-conductive epicardial mesh. Science Translational Medicine, 2016 8(344): p. 344ra86–344ra86.

81. Park M, et al., Highly stretchable electric circuits from a composite material of silver nanoparticles and elastomeric fibres. Nat Nano, 2012 7(12): p. 803–809.

82. Abidian MR, Corey JM, Kipke DR, Martin DC, Conducting-Polymer Nanotubes Improve Electrical Properties, Mechanical Adhesion, Neural Attachment, and Neurite Outgrowth of Neural Electrodes. Small, 2010 6(3): p. 421–429. [PubMed: 20077424]

83. Yao S and Zhu Y, Nanomaterial-Enabled Stretchable Conductors: Strategies, Materials and Devices. Advanced Materials, 2015 27(9): p. 1480–1511. [PubMed: 25619358]

84. Kirkpatrick S, Percolation and Conduction. Reviews of Modern Physics, 1973 45(4): p. 574–588.

85. Hu L, et al., Scalable Coating and Properties of Transparent, Flexible, Silver Nanowire Electrodes. ACS Nano, 2010 4(5): p. 2955–2963. [PubMed: 20426409]

86. Perlmutter JS and Mink JW, Deep brain stimulation. Annual review of neuroscience, 2006 29: p. 229–57.

87. North RB, et al., Spinal cord stimulation for chronic, intractable pain: Superiority of “multi-channel” devices. Pain, 1991 44(2): p. 119–130. [PubMed: 2052378]

88. Holtzheimer P.E.r., Mayberg HS, Deep brain stimulation for treatment-resistant depression. Am J Psychiatry, 2010 167(12): p. 1437–44. [PubMed: 21131410]

89. Cogan SF, Neural Stimulation and Recording Electrodes. Annual Review of Biomedical Engineering, 2008 10(1): p. 275–309.

90. Kringelbach ML, Jenkinson N, Owen SLF, Aziz TZ, Translational principles of deep brain stimulation. Nature reviews. Neuroscience, 2007 8(8): p. 623–635. [PubMed: 17637800]

91. Anikeeva P, Andalman AS, Witten IB, Warden MR, Goshen I, Grosenick L, Gunaydin LA, Frank L, Deisseroth K, Optetrode: a multichannel readout for optogenetic control in freely moving mice. . Nature Neuroscience, 2011 15: p. 163–170. [PubMed: 22138641]

92. Boyden ES, Zhang F, Bamberg E, Nagel G, Deisseroth K, Millisecond-timescale, genetically targeted optical control of neural activity. Nature neuroscience, 2005 8(9): p. 1263–8. [PubMed: 16116447]

93. Bruegmann T, et al., Optogenetic control of heart muscle in vitro and in vivo. Nat Meth, 2010 7(11): p. 897–900.

94. Magown P, et al., Direct optical activation of skeletal muscle fibres efficiently controls muscle contraction and attenuates denervation atrophy. Nat Commun, 2015 6.

95. Montgomery KL, et al., Beyond the brain: Optogenetic control in the spinal cord and peripheral nervous system. Science Translational Medicine, 2016 8(337): p. 337rv5–337rv5.

96. Nagel G, Szellas T, Huhn W, Kateriya S, Adeishvili N, Berthold P, Ollig D, Hegemann P, Bamberg E, Channelrhodopsin-2, a directly light-gated cation-selective membrane channel. Proceedings of the National Academy of Sciences, 2003 100(24): p. 13940–13945.

97. Zhang F, Vierock J, Yizhar O, Fenno LE, Tsunoda S, Kianianmomeni A, Prigge M, Berndt A, Cushman J, Polle J, Magnuson J, Hegemann P, Deisseroth K, The microbial opsin family of optogenetic tools. Cell, 2011 147(7): p. 1446–57. [PubMed: 22196724]

98. Zhang F, Wang LP, Brauner M, Liewald JF, Kay K, Watzke N, Wood PG, Bamberg E, Nagel G, Gottschalk A, Deisseroth K, Multimodal fast optical interrogation of neural circuitry. Nature, 2007 446(7136): p. 633–9. [PubMed: 17410168]

99. Yizhar O, Fenno LE, Davidson TJ, Mogri M, Deisseroth K, Optogenetics in neural systems. Neuron, 2011 71(1): p. 9–34. [PubMed: 21745635]

100. Klapoetke NC, Murata Y, Kim SS, Pulver SR, Birdsey-Benson A, Cho YK, Morimoto TK, Chuong AS, Carpenter EJ, Tian Z, Wang J, Xie Y, Yan Z, Zhang Y, Chow BY, Surek B, Melkonian M, Jayaraman V, Constantine-Paton M, Wong GK-S, Boyden ES, Independent optical excitation of distinct neural populations. Nat Meth, 2014 11(3): p. 338–346.

101. Zhang J, Laiwalla F, Kim JA, Urabe H, Van Wagenen R, Song YK, Connors BW, Zhang F, Deisseroth K, Nurmikko AV, Integrated device for optical stimulation and spatiotemporal electrical recording of neural activity in light-sensitized brain tissue. Journal of Neural Engineering, 2009 6(5): p. 055007. [PubMed: 19721185]

102. Royer S, Zemelman BV, Barbic M, Losonczy A, Buzsaki G, Magee JC, Multi-array silicon probes with integrated optical fibers: light-assisted perturbation and recording of local neural

circuits in the behaving animal. European Journal of Neuroscience, 2010 31(12): p. 2279–91. [PubMed: 20529127]

103. Kravitz AV, Owen SF, Kreitzer AC, Optogenetic identification of striatal projection neuron subtypes during in vivo recordings. Brain Research, 2013 1511(0): p. 21–32. [PubMed: 23178332]
104. Buzsáki G, Stark E, Berényi A, Khodagholy D, Kipke DR, Yoon E, Wise KD, Tools for Probing Local Circuits: High-Density Silicon Probes Combined with Optogenetics. Neuron, 2015 86(1): p. 92–105. [PubMed: 25856489]
105. Wu F, Stark E, Ku P-C, Wise KD, Buzsáki G, Yoon E, Monolithically Integrated μLEDs on Silicon Neural Probes for High-Resolution Optogenetic Studies in Behaving Animals. Neuron, 2015 88(6): p. 1136–1148. [PubMed: 26627311]
106. Lee J, Ozden I, Song Y-K, Nurmikko AV, Transparent intracortical microprobe array for simultaneous spatiotemporal optical stimulation and multichannel electrical recording. Nat. Meth, 2015 12(12): p. 1157–1162.
107. Kuzum D, et al., Transparent and flexible low noise graphene electrodes for simultaneous electrophysiology and neuroimaging. Nat Commun, 2014 5.
108. Rubehn B, Wolff SB, Tovote P, Lüthi A, Stieglitz T, A polymer-based neural microimplant for optogenetic applications: design and first in vivo study. Lab on Chip, 2013 13(4): p. 579–88.
109. Kim TI, McCall JG, Jung YH, Huang X, Siuda ER, Li Y, Song J, Song YM, Pao HA, Kim RH, Lu C, Lee SD, Song IS, Shin G, Al-Hasani R, Kim S, Tan MP, Huang Y, Omenetto FG, Rogers JA, Bruchas MR, Injectable, cellular-scale optoelectronics with applications for wireless optogenetics. Science, 2013 340(6129): p. 211–6. [PubMed: 23580530]
110. van den Brand R, et al., Restoring Voluntary Control of Locomotion after Paralyzing Spinal Cord Injury. Science, 2012 336(6085): p. 1182–1185. [PubMed: 22654062]
111. Urban DJ and Roth BL, DREADDs (Designer Receptors Exclusively Activated by Designer Drugs): Chemogenetic Tools with Therapeutic Utility. Annual Review of Pharmacology and Toxicology, 2015 55(1): p. 399–417.
112. Jeong J-W, et al., Wireless Optofluidic Systems for Programmable In Vivo Pharmacology and Optogenetics. Cell, 2015 162(3): p. 662–674. [PubMed: 26189679]
113. Muller R, et al., A Minimally Invasive 64-Channel Wireless μECoG Implant. IEEE Journal of Solid-State Circuits, 2015 50(1): p. 344–359.
114. Montgomery KL, et al., Wirelessly powered, fully internal optogenetics for brain, spinal and peripheral circuits in mice. Nat Meth, 2015 12(10): p. 969–974.
115. Park SI, et al., Soft, stretchable, fully implantable miniaturized optoelectronic systems for wireless optogenetics. Nat Biotech, 2015 33(12): p. 1280–1286.
116. Seo D, et al., Model validation of untethered, ultrasonic neural dust motes for cortical recording. Journal of Neuroscience Methods, 2015 244: p. 114–122. [PubMed: 25109901]
117. Seo D, et al., Wireless Recording in the Peripheral Nervous System with Ultrasonic Neural Dust. Neuron, 2016 91(3): p. 529–539. [PubMed: 27497221]
118. Spira ME and Hai A, Multi-electrode array technologies for neuroscience and cardiology. Nat Nano, 2013 8(2): p. 83–94.
119. Shmoel N, et al., Multisite electrophysiological recordings by self-assembled loose-patch-like junctions between cultured hippocampal neurons and mushroom-shaped microelectrodes. Scientific Reports, 2016 6: p. 27110. [PubMed: 27256971]
120. Kang M, et al., Subcellular Neural Probes from Single-Crystal Gold Nanowires. ACS Nano, 2014 8(8): p. 8182–8189. [PubMed: 25112683]
121. Robinson JT, et al., Vertical nanowire electrode arrays as a scalable platform for intracellular interfacing to neuronal circuits. Nat Nano, 2012 7(3): p. 180–184.
122. Xie C, et al., Intracellular recording of action potentials by nanopillar electroporation. Nat Nano, 2012 7(3): p. 185–190.
123. Lin ZC, et al., Iridium oxide nanotube electrodes for sensitive and prolonged intracellular measurement of action potentials. Nat Commun, 2014 5.

124. Almquist BD and Melosh NA, Fusion of biomimetic stealth probes into lipid bilayer cores. Proceedings of the National Academy of Sciences, 2010 107(13): p. 5815–5820.
125. Patolsky F, et al., Detection, Stimulation, and Inhibition of Neuronal Signals with High-Density Nanowire Transistor Arrays. Science, 2006 313(5790): p. 1100–1104. [PubMed: 16931757]
126. Tian B and Lieber CM, Synthetic Nanoelectronic Probes for Biological Cells and Tissues. Annual Review of Analytical Chemistry, 2013 6(1): p. 31–51.
127. Duan X, et al., Intracellular recordings of action potentials by an extracellular nanoscale field-effect transistor. Nat Nano, 2012 7(3): p. 174–179.
128. Tian B, et al., Three-dimensional, flexible nanoscale field-effect transistors as localized bioprobes. Science, 2010 329(5993): p. 830–834. [PubMed: 20705858]
129. Liu J, et al., Syringe-injectable electronics. Nat Nano, 2015 10(7): p. 629–636.
130. Xie C, et al., Three-dimensional macroporous nanoelectronic networks as minimally invasive brain probes. Nat Mater, 2015 14(12): p. 1286–1292. [PubMed: 26436341]
131. Fu T-M, et al., Stable long-term chronic brain mapping at the single-neuron level. Nat Meth, 2016 13: p. 875–882.
132. Wang Y and Guo L, Nanomaterial-Enabled Neural Stimulation. Frontiers in Neuroscience, 2016 10: p. 69. [PubMed: 27013938]
133. Gao J, Gu H, and Xu B, Multifunctional Magnetic Nanoparticles: Design, Synthesis, and Biomedical Applications. Accounts of Chemical Research, 2009 42(8): p. 1097–1107. [PubMed: 19476332]
134. Hu M, et al., Gold nanostructures: engineering their plasmonic properties for biomedical applications. Chemical Society Reviews, 2006 35(11): p. 1084–1094. [PubMed: 17057837]
135. Luan S, et al., Neuromodulation: present and emerging methods. Frontiers in Neuroengineering, 2014 7.
136. Wells J, et al., Application of infrared light for in vivo neural stimulation. Journal of Biomedical Optics, 2005 10(6): p. 064003-064003-12.
137. Yizhar O, et al., Optogenetics in Neural Systems. Neuron, 2011 71(1): p. 9–34. [PubMed: 21745635]
138. Aravanis AM, Wang LP, Zhang F, Meltzer LA, Mogri MZ, Schneider MB, Deisseroth K, An optical neural interface: in vivo control of rodent motor cortex with integrated fiberoptic and optogenetic technology. Journal of Neural Engineering, 2007 4(3): p. S143–56. [PubMed: 17873414]
139. Knopfel T, Genetically encoded optical indicators for the analysis of neuronal circuits. Nature reviews. Neuroscience, 2012 13(10): p. 687–700. [PubMed: 22931891]
140. Horton NG, et al., In vivo three-photon microscopy of subcortical structures within an intact mouse brain. Nat Photon, 2013 7(3): p. 205–209.
141. Han F.f. and Hu J.h.. Distribution and strength of sound in the human head. in Piezoelectricity, Acoustic Waves, and Device Applications (SPAWDA), 2015 Symposium on. 2015.
142. Bystritsky A and Korb A, A Review of Low-Intensity Transcranial Focused Ultrasound for Clinical Applications. Current Behavioral Neuroscience Reports, 2015 2(2): p. 60–66.
143. Legon W, et al., Transcranial focused ultrasound modulates the activity of primary somatosensory cortex in humans. Nat Neurosci, 2014 17(2): p. 322–329. [PubMed: 24413698]
144. Mace E, et al., Functional ultrasound imaging of the brain. Nat Meth, 2011 8(8): p. 662–664.
145. Bottomley PA and Andrew ER, RF magnetic field penetration, phase shift and power dissipation in biological tissue: implications for NMR imaging. Physics in Medicine and biology, 1978 23(4): p. 630. [PubMed: 704667]
146. Young JH, Wang MT, and Brezovich IA, Frequency/depth-penetration considerations in hyperthermia by magnetically induced currents. Electronics Letters, 1980 16(10): p. 358–359.
147. Hallett M, Transcranial Magnetic Stimulation: A Primer. Neuron, 2007 55(2): p. 187–199. [PubMed: 17640522]
148. Deng Z-D, Lisanby SH, and Peterchev AV, Electric field depth–focality tradeoff in transcranial magnetic stimulation: Simulation comparison of 50 coil designs. Brain Stimulation, 2013 6(1): p. 1–13. [PubMed: 22483681]

149. Matthews PM, Honey GD, and Bullmore ET, Applications of fMRI in translational medicine and clinical practice. Nat Rev Neurosci, 2006 7(9): p. 732–744. [PubMed: 16924262]

150. Wang Y and Guo L, Nanomaterial-enabled neural stimulation. Frontiers in Neuroscience, 2016 10.

151. Errico C, et al., Ultrafast ultrasound localization microscopy for deep super-resolution vascular imaging. Nature, 2015 527(7579): p. 499–502. [PubMed: 26607546]

152. Cho MH, et al., A magnetic switch for the control of cell death signalling in in vitro and in vivo systems. Nat Mater, 2012 11(12): p. 1038–1043. [PubMed: 23042417]

153. Lee J-H, et al., Magnetic Nanoparticles for Ultrafast Mechanical Control of Inner Ear Hair Cells. ACS Nano, 2014 8(7): p. 6590–6598. [PubMed: 25004005]

154. Pankhurst QA, Thanh NTK, Jones SK, Dobson J, Progress in applications of magnetic nanoparticles in biomedicine. Journal of Physics D: Applied Physics, 2009 42(22): p. 224001 1–15.

155. Guduru R, et al., Magneto-electric Nanoparticles to Enable Field-controlled High-Specificity Drug Delivery to Eradicate Ovarian Cancer Cells. Sci. Rep, 2013 3.

156. Lugo K, et al., Remote switching of cellular activity and cell signaling using light in conjunction with quantum dots. Biomedical Optics Express, 2012 3(3): p. 447–454. [PubMed: 22435093]

157. Pappas TC, et al., Nanoscale Engineering of a Cellular Interface with Semiconductor Nanoparticle Films for Photoelectric Stimulation of Neurons. Nano Letters, 2007 7(2): p. 513–519. [PubMed: 17298018]

158. Rowland CE, et al., Electric Field Modulation of Semiconductor Quantum Dot Photoluminescence: Insights Into the Design of Robust Voltage-Sensitive Cellular Imaging Probes. Nano Letters, 2015 15(10): p. 6848–6854. [PubMed: 26414396]

159. Marshall JD and Schnitzer MJ, Optical Strategies for Sensing Neuronal Voltage Using Quantum Dots and Other Semiconductor Nanocrystals. ACS Nano, 2013 7(5): p. 4601–4609. [PubMed: 23614672]

160. Derfus AM, Chan WC, and Bhatia SN, Probing the cytotoxicity of semiconductor quantum dots. Nano letters, 2004 4(1): p. 11–18. [PubMed: 28890669]

161. Murphy CJ, et al., Gold Nanoparticles in Biology: Beyond Toxicity to Cellular Imaging. Accounts of Chemical Research, 2008 41(12): p. 1721–1730. [PubMed: 18712884]

162. Yoo S, et al., Photothermal Inhibition of Neural Activity with Near-Infrared-Sensitive Nanotransducers. ACS Nano, 2014 8(8): p. 8040–8049. [PubMed: 25046316]

163. Carvalho-de-Souza João L., et al., Photosensitivity of Neurons Enabled by Cell-Targeted Gold Nanoparticles. Neuron. 86(1): p. 207–217. [PubMed: 25772189]

164. Lavoie-Cardinal F, et al., Gold nanoparticle-assisted all optical localized stimulation and monitoring of Ca2+ signaling in neurons. Scientific Reports, 2016 6: p. 20619. [PubMed: 26857748]

165. Nakatsuji H, et al., Thermosensitive Ion Channel Activation in Single Neuronal Cells by Using Surface-Engineered Plasmonic Nanoparticles. Angewandte Chemie International Edition, 2015 54(40): p. 11725–11729. [PubMed: 26249533]

166. Zhang J, Atay T, and Nurmikko AV, Optical Detection of Brain Cell Activity Using Plasmonic Gold Nanoparticles. Nano Letters, 2009 9(2): p. 519–524. [PubMed: 19199762]

167. Juluri BK, et al., Effects of Geometry and Composition on Charge-Induced Plasmonic Shifts in Gold Nanoparticles. The Journal of Physical Chemistry C, 2008 112(19): p. 7309–7317.

168. Kucsko G, Maurer PC, Yao NY, Kubo M, Noh HJ, Lo PK, Park H, Lukin MD, Nanometre-scale thermometry in a living cell. Nature, 2013 500(7460): p. 54–8. [PubMed: 23903748]

169. Karaveli S, et al., Modulation of nitrogen vacancy charge state and fluorescence in nanodiamonds using electrochemical potential. Proceedings of the National Academy of Sciences, 2016 113(15): p. 3938–3943.

170. Barry J, et al., Optical magnetic detection of single-neuron action potentials using quantum defects in diamond. arXiv preprint arXiv:160201056, 2016.

171. Zhang Y, et al., Illuminating Cell Signaling with Near-Infrared Light-Responsive Nanomaterials. ACS nano, 2016 10(4): p. 3881–3885. [PubMed: 27077481]

172. He L, et al., Near-infrared photoactivatable control of Ca2+ signaling and optogenetic immunomodulation. eLife, 2015 4: p. e10024. [PubMed: 26646180]
173. Ibsen S, et al., Sonogenetics is a non-invasive approach to activating neurons in Caenorhabditis elegans. Nat Commun, 2015 6.
174. Marino A, et al., Piezoelectric Nanoparticle-Assisted Wireless Neuronal Stimulation. ACS Nano, 2015 9(7): p. 7678–7689. [PubMed: 26168074]
175. Dobson J, Remote control of cellular behaviour with magnetic nanoparticles. Nat Nano, 2008 3(3): p. 139–143.
176. Ingber DE, Cellular mechanotransduction: putting all the pieces together again. The FASEB Journal, 2006 20(7): p. 811–827. [PubMed: 16675838]
177. Seo D, et al., A Mechanogenetic Toolkit for Interrogating Cell Signaling in Space and Time. Cell. 165(6): p. 1507–1518.
178. Hughes S, et al., Selective activation of mechanosensitive ion channels using magnetic particles. Journal of the Royal Society Interface, 2008 5(25): p. 855–863.
179. Hoffmann C, et al., Spatiotemporal control of microtubule nucleation and assembly using magnetic nanoparticles. Nature nanotechnology, 2013 8(3): p. 199–205.
180. Kim D-H, et al., Biofunctionalized magnetic-vortex microdiscs for targeted cancer-cell destruction. Nat Mater, 2010 9(2): p. 165–171. [PubMed: 19946279]
181. Mannix RJ, et al., Nanomagnetic actuation of receptor-mediated signal transduction. Nat Nano, 2008 3(1): p. 36–40.
182. Carrey J, Mehdaoui B, and Respaud M, Simple Models for Dynamic Hysteresis Loop Calculations of Magnetic Single-domain Nanoparticles: Application to Magnetic Hyperthermia Optimization. Journal of Applied Physics, 2011 109(8): p. 083921–17.
183. Chen R, et al., Wireless magnetothermal deep brain stimulation. Science, 2015 347(6229): p. 1477–1480. [PubMed: 25765068]
184. Huang H, et al., Remote Control of Ion Channels and Neurons through Magnetic-Field Heating of Nanoparticles, in Nature Nanotechnology. 2010 p. 602–606.
185. Stanley SA, et al., Radio-Wave Heating of Iron Oxide Nanoparticles Can Regulate Plasma Glucose in Mice. Science, 2012 336(6081): p. 604–608. [PubMed: 22556257]
186. Nair M, et al., Externally controlled on-demand release of anti-HIV drug using magneto-electric nanoparticles as carriers. Nat Commun, 2013 4: p. 1707. [PubMed: 23591874]
187. Guduru R, et al., Magnetoelectric'spin'on stimulating the brain. Nanomedicine, 2015 10(13): p. 2051–2061. [PubMed: 25953069]
188. Shin T-H, et al., Recent advances in magnetic nanoparticle-based multi-modal imaging. Chemical Society Reviews, 2015 44(14): p. 4501–4516. [PubMed: 25652670]
189. Davies G-L, Kramberger I, and Davis JJ, Environmentally responsive MRI contrast agents. Chemical Communications, 2013 49(84): p. 9704–9721. [PubMed: 24040650]
190. Atanasijevic T, et al., Calcium-sensitive MRI contrast agents based on superparamagnetic iron oxide nanoparticles and calmodulin. Proceedings of the National Academy of Sciences of the United States of America, 2006 103(40): p. 14707–14712. [PubMed: 17003117]
191. Shapiro MG, et al., Dynamic imaging with MRI contrast agents: quantitative considerations. Magnetic Resonance Imaging, 2006 24(4): p. 449–462. [PubMed: 16677952]
192. Rodriguez E, et al., Magnetic nanosensors optimized for rapid and reversible self-assembly. Chemical Communications, 2014 50(27): p. 3595–3598. [PubMed: 24566735]
193. Lee T, Cai LX, Lelyveld VS, Hai A, Jasanoff A, Molecular-Level Functional Magnetic Resonance Imaging of Dopaminergic Signaling. Science, 2014 344(6183): p. 533–535. [PubMed: 24786083]
194. Christiansen MG, et al., Magnetically multiplexed heating of single domain nanoparticles. Applied Physics Letters, 2014 104(21): p. −.
195. Wijaya A, et al., Selective release of multiple DNA oligonucleotides from gold nanorods. Acs Nano, 2008 3(1): p. 80–86.
196. Chen R, Christiansen MG, Sourakov A, Mohr A, Matsumoto Y, Okada S, Jasanoff A, Anikeeva P, High-Performance Ferrite Nanoparticles through Nonaqueous Redox Phase Tuning. Nano Letters, 2016 16(2): p. 1345–1351. [PubMed: 26756463]

197. Chen Y and Liu L, Modern methods for delivery of drugs across the blood–brain barrier. Advanced Drug Delivery Reviews, 2012 64(7): p. 640–665. [PubMed: 22154620]

198. Salvati A, et al., Transferrin-functionalized nanoparticles lose their targeting capabilities when a biomolecule corona adsorbs on the surface. Nature Nanotechnology, 2013 8(2): p. 137–143.

199. Tenzer S, et al., Rapid formation of plasma protein corona critically affects nanoparticle pathophysiology. Nature Nanotechnology, 2013 8(10): p. 772–781.

200. Kim JA, et al., Role of cell cycle on the cellular uptake and dilution of nanoparticles in a cell population. Nature nanotechnology, 2012 7(1): p. 62–68.

201. Hynynen K, et al., Local and reversible blood–brain barrier disruption by noninvasive focused ultrasound at frequencies suitable for trans-skull sonications. Neuroimage, 2005 24(1): p. 12–20. [PubMed: 15588592]

202. Chertok B, et al., Iron oxide nanoparticles as a drug delivery vehicle for MRI monitored magnetic targeting of brain tumors. Biomaterials, 2008 29(4): p. 487–496. [PubMed: 17964647]

203. van Landeghem FKH, et al., Post-mortem studies in glioblastoma patients treated with thermotherapy using magnetic nanoparticles. Biomaterials, 2009 30(1): p. 52–57. [PubMed: 18848723]

204. Tang, Jonathan CY, et al., A Nanobody-Based System Using Fluorescent Proteins as Scaffolds for Cell-Specific Gene Manipulation. Cell, 2013 154(4): p. 928–939. [PubMed: 23953120]

205. Antman-Passig M and Shefi O, Remote Magnetic Orientation of 3D Collagen Hydrogels for Directed Neuronal Regeneration. Nano Letters, 2016 16(4): p. 2567–2573. [PubMed: 26943183]

206. Malgosia MP, Brian GB, and Molly SS, Injectable hydrogels for central nervous system therapy. Biomedical Materials, 2012 7(2): p. 024101. [PubMed: 22456684]

207. Shapiro MG, et al., Biogenic gas nanostructures as ultrasonic molecular reporters. Nat Nano, 2014 9(4): p. 311–316.

208. Stanley SA, et al., Bidirectional electromagnetic control of the hypothalamus regulates feeding and metabolism. Nature, 2016 531(7596): p. 647–650. [PubMed: 27007848]

209. Wheeler MA, et al., Genetically targeted magnetic control of the nervous system. Nature neuroscience, 2016 19: p. 756–761. [PubMed: 26950006]

210. Chasteen ND and Harrison PM, Mineralization in Ferritin: An Efficient Means of Iron Storage. Journal of Structural Biology, 1999 126(3): p. 182–194. [PubMed: 10441528]

211. Meister M, Physical limits to magnetogenetics. eLife, 2016 5: p. e17210. [PubMed: 27529126]

212. Komeili A, et al., Magnetosomes are cell membrane invaginations organized by the actin-like protein MamK. Science, 2006 311(5758): p. 242–245. [PubMed: 16373532]

213. Kolinko I, et al., Biosynthesis of magnetic nanostructures in a foreign organism by transfer of bacterial magnetosome gene clusters. Nat Nano, 2014 9(3): p. 193–197.

214. French DD, et al., Health Care Costs for Patients With Chronic Spinal Cord Injury in the Veterans Health Administration. The Journal of Spinal Cord Medicine, 2007 30(5): p. 477–481. [PubMed: 18092564]

215. Kowal SL, et al., The current and projected economic burden of Parkinson's disease in the United States. Mov Disord, 2013 28(3): p. 311–8. [PubMed: 23436720]

216. Calabresi P, et al., Direct and indirect pathways of basal ganglia: a critical reappraisal. Nat Neurosci, 2014 17(8): p. 1022–1030. [PubMed: 25065439]

217. Arber S, Motor circuits in action: specification, connectivity, and function. Neuron, 2012 74(6): p. 975–89. [PubMed: 22726829]

218. Holstege G, Descending motor pathways and the spinal motor system: Limbic and nonlimbic components. Progress in brain research, 1991 87: p. 307–421. [PubMed: 1678191]

219. Hammerle H, et al., Biostability of micro-photodiode arrays for subretinal implantation. Biomaterials, 2002 23(3): p. 797–804. [PubMed: 11771699]

220. Patrick E, et al., Corrosion of tungsten microelectrodes used in neural recording applications. Journal of Neuroscience Methods, 2011 198(2): p. 158–171. [PubMed: 21470563]

221. Wang A, et al., Stability of and inflammatory response to silicon coated with a fluoroalkyl self-assembled monolayer in the central nervous system. Journal of Biomedical Materials Research Part A, 2007 81A(2): p. 363–372.

222. Li W, et al., Corrosion Behavior of Parylene-Metal-Parylene Thin Films in Saline. ECS Transactions, 2008 11(18): p. 1–6.

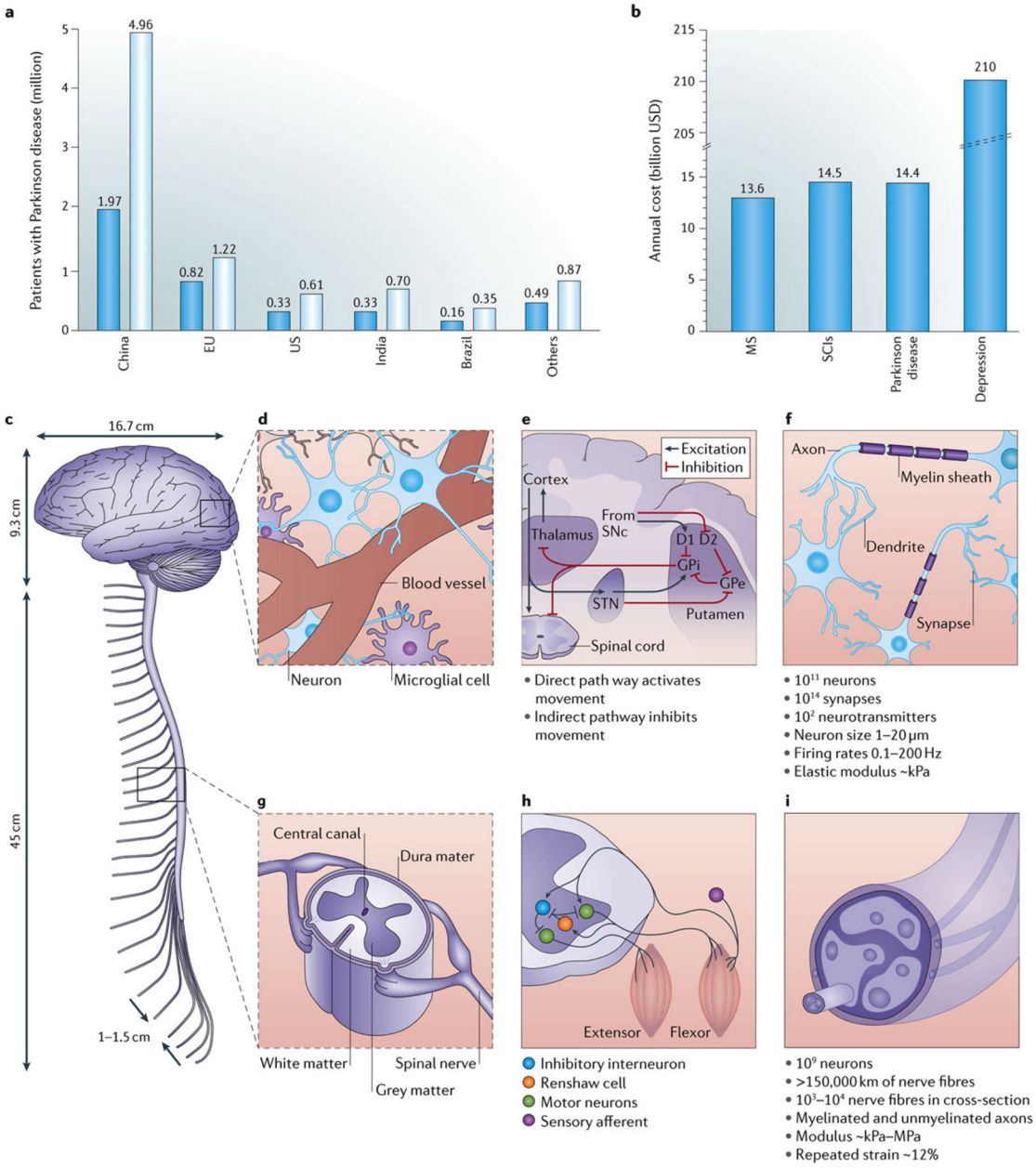

Figure 1 | . Challenges of designing for the nervous system.

a | The worldwide population of diagnosed Parkinson's disease cases in 2005 (4.1 million) and the corresponding projection to 2030 (8.7 million) [1]. **b** | Combined annual cost of multiple sclerosis [2], spinal cord injuries [214], Parkinson's disease [215], and depression [3] in the US displayed in US$ billions. **c** | Dimensions of the brain and spinal cord. **d** | Brain tissue encompassing neurons, glia and blood vessels. **e** | Circuit diagram for direct and indirect motor pathways in the brain [216]. f | Physiological facts pertaining to brain function. **g** | Spinal-cord cross-section. **h** | Circuit diagram of motor pathway in the spinal cord [217, 218]. **i** | Cross-sectional diagram of a peripheral nerve. Physiological facts pertaining to the spinal-cord and peripheral-nerve function [10]. SNc, substantial nigra pars

compacta; GPi, internal external globus palidus; GPe, internal globus palidus; STN, subthalamic nucleus; D1 and D2, dopamine receptors.

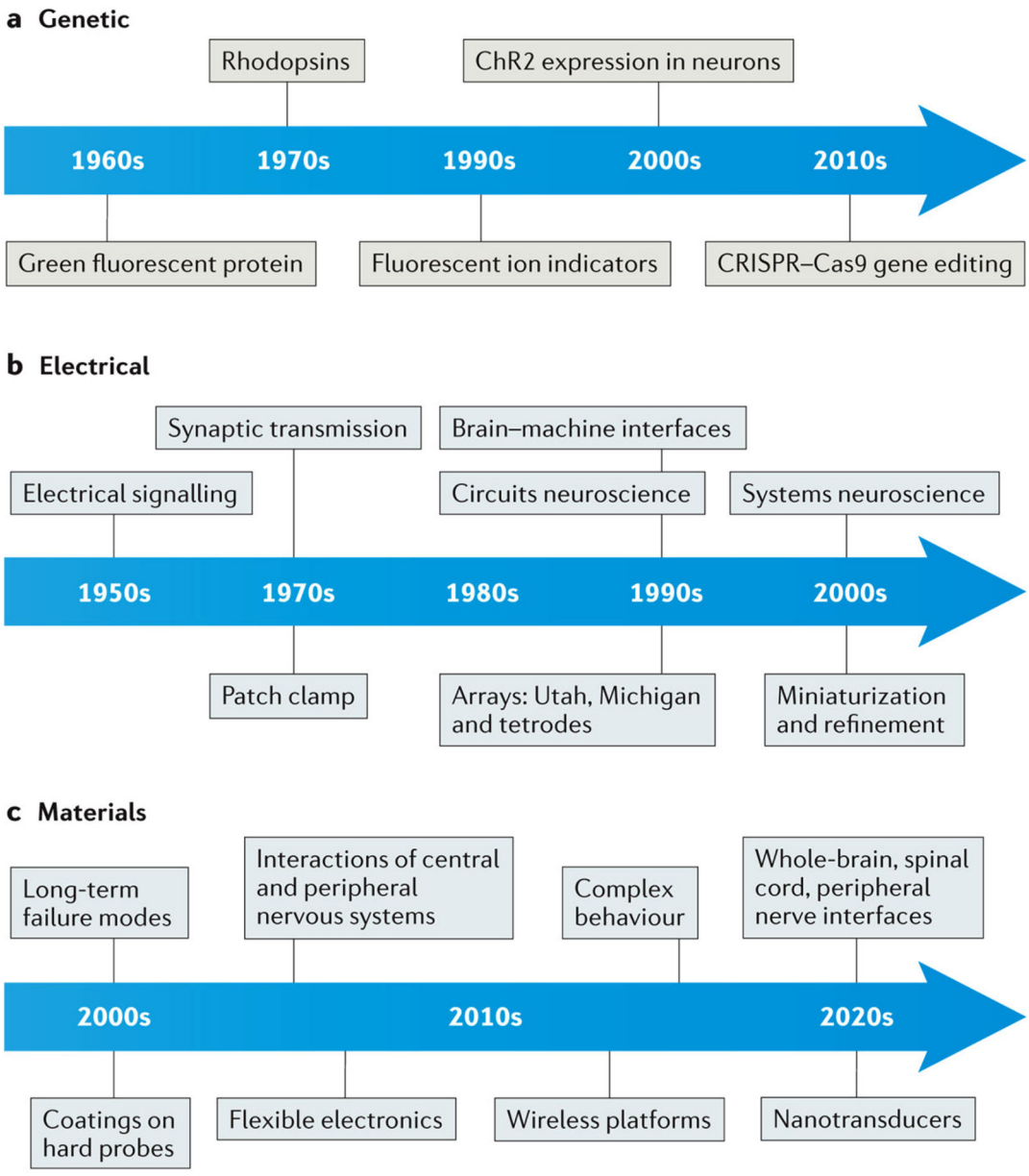

Figure 2 | . Historical view of neural interface research.

Progress in genetic tools for imagining and manipulating neural circuits paralleled engineering trends in neural probe design. The development of neural interfaces, driven by the needs of brain–machine interface research, has been confounded by the failure of neural probes in chronic long-term experiments. Recently, there has been a materials-driven pursuit to reduce the foreign-body response, push the resolution of neural interfaces to sub-cellular dimensions and integrate the capabilities required for deployment of genetic tools.

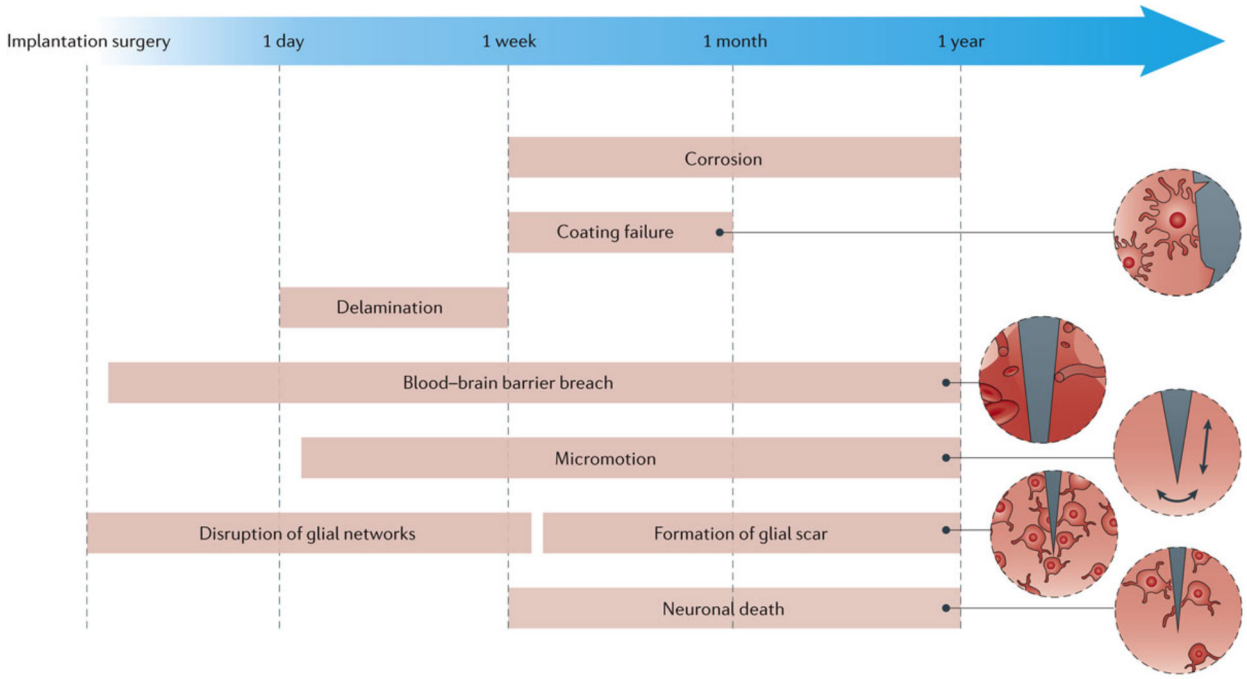

Figure 3 | . Mechanisms of neural-probe failure.

Failure modes of neural probes manifested as a loss of neural recording capability can be classified into those relating to device design [29, 35] (above the arrow) and foreign-body response [34, 36] (below the arrow). Design failure mechanisms include mechanical failure of interconnects [35], degradation and cracking of the insulation [219], electrode corrosion [220, 221] and delamination of probe layers [222]. Biological failure mechanisms include initial tissue damage during insertion [34, 37]; breach of the blood–brain barrier [41]; elastic mismatch and tissue micromotion [35, 38, 39]; disruption of glial networks [40]; formation of a glial scar; and neuronal death associated with the abovementioned factors, as well as with materials neurotoxicity [42] and chemical mismatch [34].

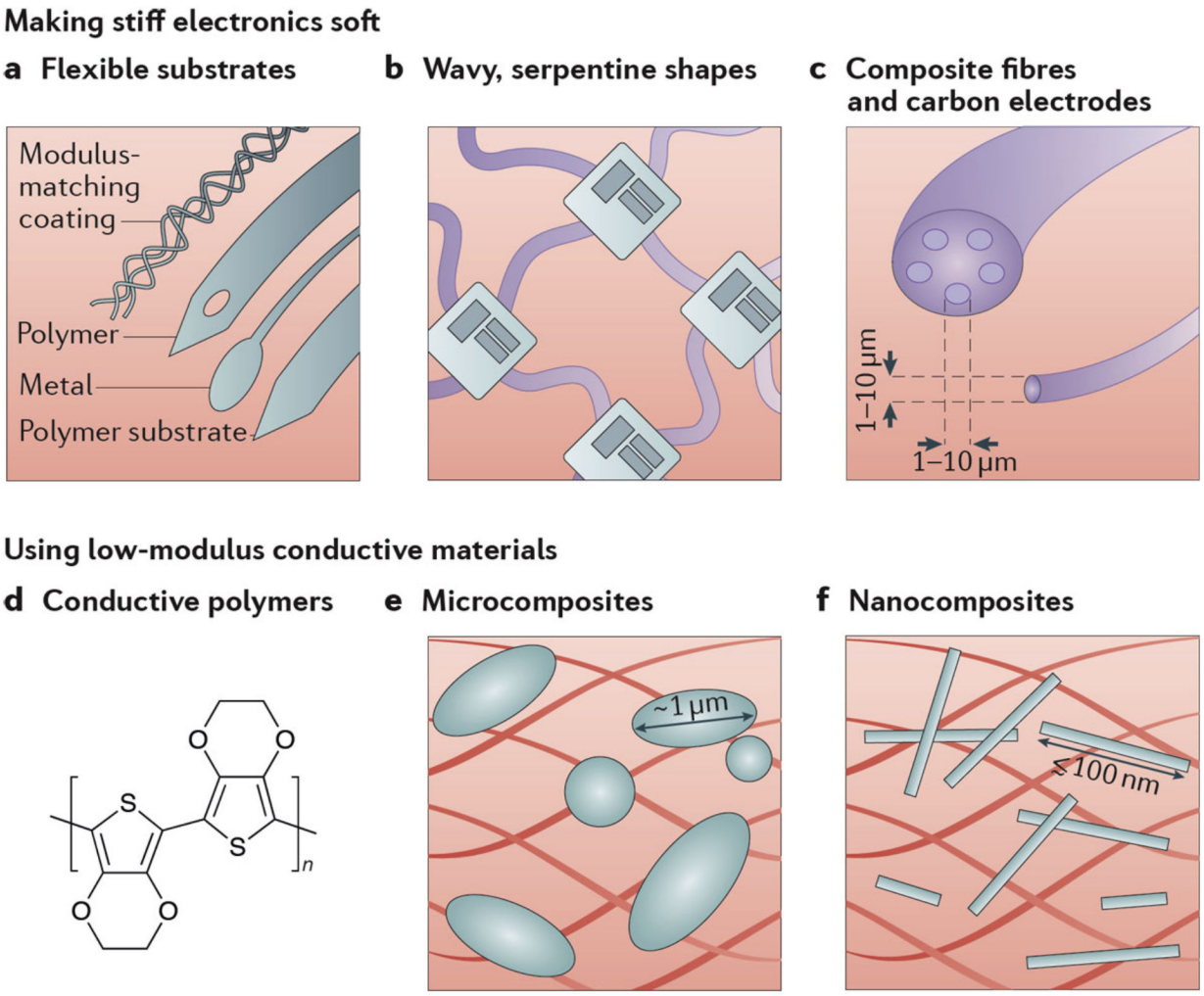

Figure 4 | . Examples of approaches intended to overcome foreign-body response and increase the resolution of neural interfaces.

a | Use of flexible substrates and modulus-matching coatings to reduce elastic mismatch between the neural probes and neural tissues. **b** | Contact-printed serpentine, wavy, and fractal interconnects. **c** | Thermally drawn fibers with micron-scale electrodes and carbon-fiber microelectrodes. **d** | Conductive polymers used as flexible alternatives to crystalline semiconductors and metals. **e,f** | Conductive composites of flexible and stretchable polymers and carbon and metal micro- and nanoparticles.

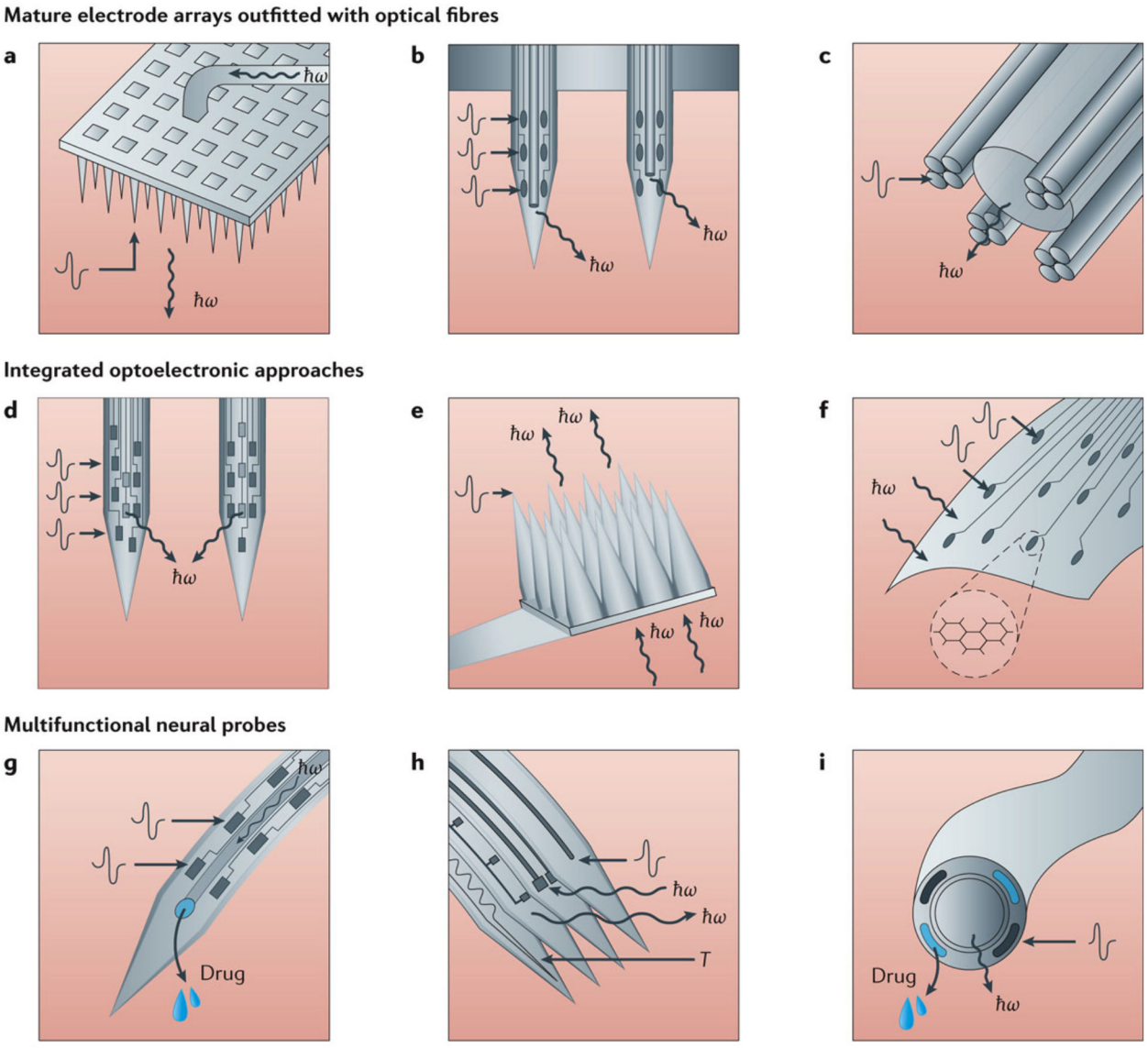

Figure 5 | . Probes for bi-directional communication with neural circuits.

a–c | Integration of optical fibers into Utah arrays [101], Michigan probes [102] and tetrodes [91], respectively, intended for optogenetics research. **d** | Gallium-nitride-based micro-LEDs monolithically integrated onto silicon substrates within Michigan-style probes [105]. **e** | Transparent multi-electrode arrays composed of conductive ZnO [106]. **f** | Transparent and flexible arrays of graphene surface electrodes [107]. **g** | MEMS-processed tri-functional polymer probe integrating an SU-8 waveguide, metal electrodes and a microfluidic channel on a polyimide substrate [108]. **h** | Multifunctional microcontact printed probe containing an electrode, micro LEDs, a photodetector and a thermistor [109]. **i** | Multifunctional all-polymer fiber-probe integrating a waveguide, carbon composite electrodes and microfluidic channels [65]. LED, light-emitting device.

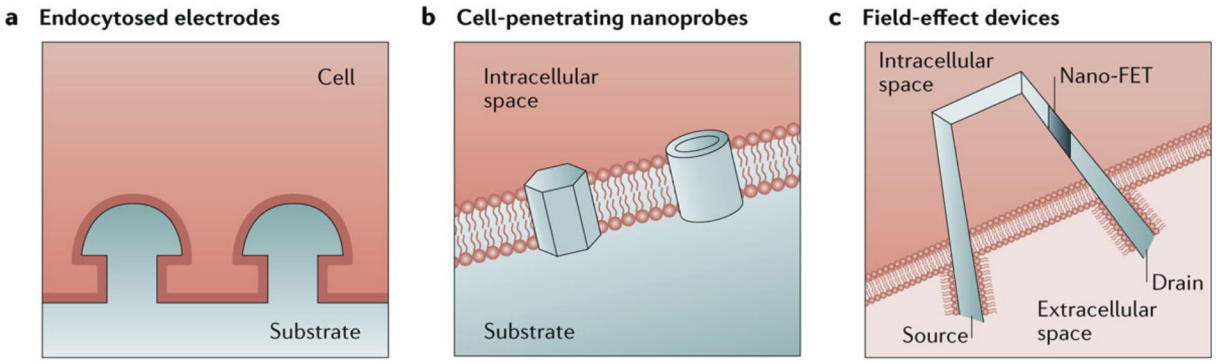

Figure 6 | . Micro- and nanoprobes for intracellular recordings.

a | Endocytosed mushroom electrodes for high-SNR recordings [118, 119]. **b** | Cell-penetrating nanopillar [122], nanowire [121], and nano-straw electrodes [123]. **c** | Field-effect devices based on kinked semiconductor nanowires. [129–131]. SNR, signal-to-noise ratio.

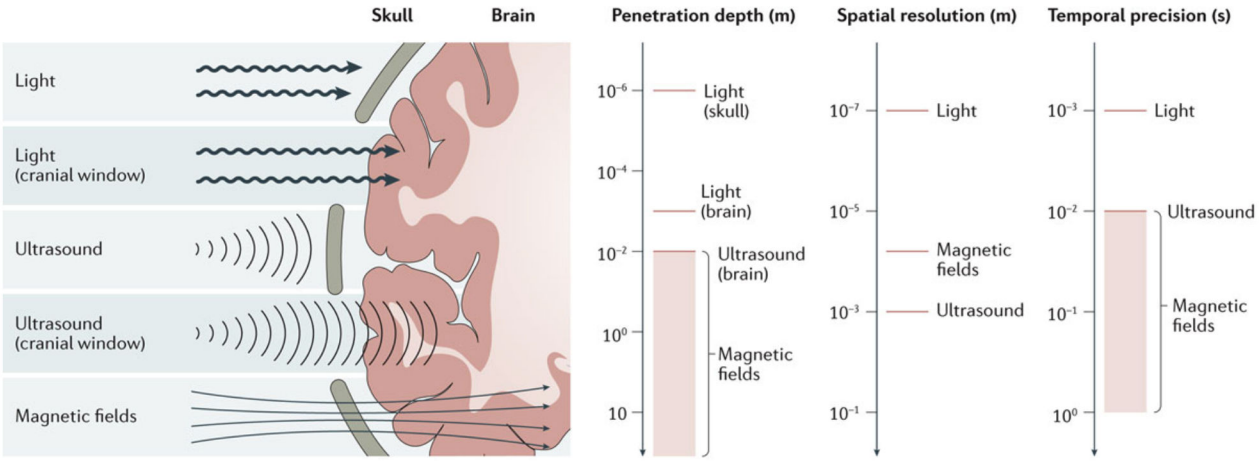

Figure 7 | . Tissue penetration by optical, ultrasonic and magnetic signals.

Electromagnetic waves in the visible and (near) infrared optical spectrum afford superior spatial and temporal resolution but limited penetration depth (~1–1.5 mm) [137, 140]. Ultrasound can access deeper brain regions (>50 mm), with a spatial resolution that is inversely proportional to the wavelength, which in turn scales inversely with the penetration depth (in general for ultrasound spatial resolution is > 1 mm^3, temporal precision >10 ms) [143]. Alternating magnetic fields (AMFs) with low frequencies (<1 kHz) and high amplitudes (0.1–2 T) inductively couple to the upper 1–10 mm of tissue [147]. AMFs with amplitudes of ~1–100 mT and frequencies in the low radiofrequency range (0.1–1 MHz) travel through tissue unaffected [146]. Temporal precision of neural activity is dependent on the chosen magnetic scheme.

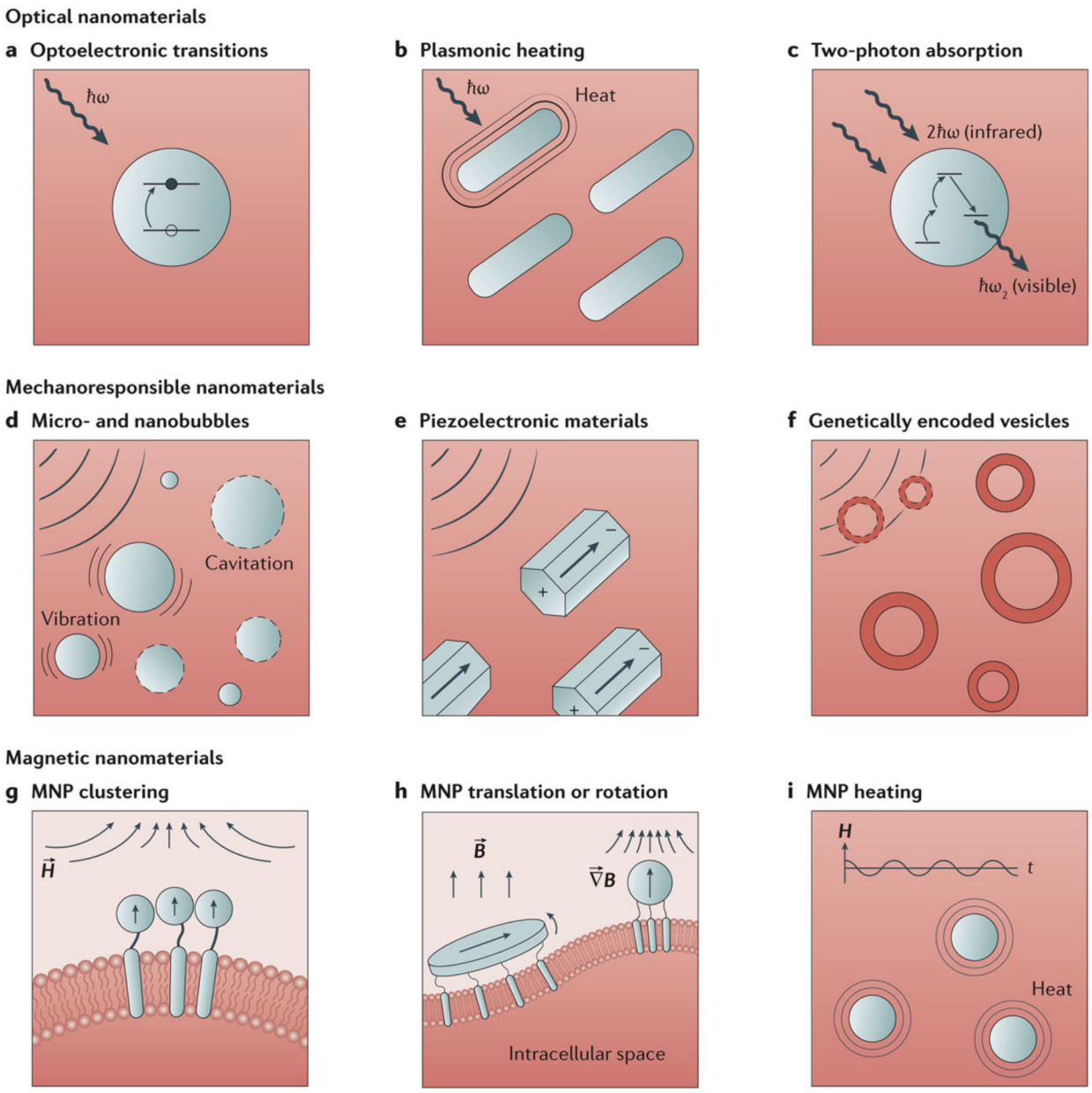

Figure 8 | . Nanomaterials as local transducers of external stimuli.

a | Optoelectronic transitions in semiconductor quantum dots can be used to convert optical stimuli into electrical signals and *vice versa*, which can enable stimulation and recording of neural activity [156–159]. **b** | Metallic nanoparticles couple to visible and near-infrared light through their plasmon resonance [134]. Plasmon energy is dissipated as heat, which can be used to modulate membrane capacitance or trigger heat-sensitive ion-channels in neurons [162, 163]. Plasmon resonance is also sensitive to electric fields, and can be used to detect changes in neuronal membrane voltage [166]. **c** | Upconversion nanoparticles convert infrared to visible light via a two-photon absorption process. This effect may extend the penetration depth of optical neuromodulation techniques [172]. **d** | Vibration, rotation and cavitation processes in hollow micro- and nanobubbles may induce action-potential

firing in targeted neurons at ultrasound intensities otherwise insufficient to evoke excitation [173]. Microbubbles can also improve the resolution of functional ultrasound imaging by acting as contrast agents [151]. **e** | Mechanical deformation by ultrasound can polarize piezoelectric nanomaterials for localized electrical stimulation [174]. **f** | Genetically encoded gas vesicles function similarly to synthetic inert gas micro- and nanobubbles [207]. **g** | Clustering of magnetic nanoparticles in time-constant magnetic-field gradients can be used to control membrane-protein complexes and influence cell fate [152]. **h** | In slowly varying magnetic fields, magnetic nanodisks exert torque on the cell membrane [180] and magnetic nanoparticles exert tensile force. These mechanical cues can trigger the opening of mechanosensitive ion channels [175]. **i** | Hysteretic heating of magnetic nanoparticles exposed to alternating magnetic fields triggers heat-sensitive ion channels causing Ca^{2+} influx and action-potential firing in neurons [183, 184].